Determination of Hydraulic Parameters of the Ohangwena Aquifers and Aquitards based on borehole WW203302

By

Joseph Reginalda

201169312

Thesis submitted in partial fulfillment of the Bachelor of Science Honours Degree in Geology

Supervisor: Dr. A. Wanke

Co-supervisor: Mr. C. Lohe

December 2015

Abstract

The determination of hydraulic parameters is central to aquifer studies including groundwater flow models, sustainable yield assessment and groundwater residence times. It is essential that hydraulic conductivities and effective porosities are known in their stratigraphic context. In the herein discussed study the hydraulic conductivity has been determined and evaluated for the aquifers in the Ohangwena Region based on the fully cored borehole WW203302. The borehole penetrated the Upper Kalahari Sequence to a depth to 400 meters and encountered perched and deeper confined aquifers. This study focuses on the upper 150 meters of the core. The first 8.7 meters are composed of unconsolidated sandy sediment, however the core of this uppermost interval could not be retrieved. It is known that this top interval hosts a shallow perched aquifer.

Samples have been collected in 10 meter intervals with a total of 18 samples collected. The falling head method was used to determine the hydraulic conductivity of 18 samples. With the obtained hydraulic conductivities the presence of an aquiclude with a thickness of 61.8 meters and deeper aquifer (KOH-1), just below the aquiclude, has been delineated. A borehole litholog shows that the aquifer is made of sandy material with minor silt and clay, while the fine grained fraction is significantly higher for the overlying aquitard.

Calculation of vertical groundwater movement from the shallow perched aquifer through the aquitard down to the confined aquifer KOH-1 reveals a travel time of 1096 years at a distance velocity of 5.5E-2 m/year. Such a travel time indicates that KOH-1 can receive limited recharge from the shallow perched aquifer above. The general hydrological setting allows for additional significant lateral recharge deriving from a northern source.

Dedication

This thesis is dedicated to three very important people in my life; my mom Martha Shiningayamwe, my aunt Hilja Kaholongo and my best friend Immanuel Fernando. My mom for the unconditional love and support, my aunty for understanding and caring for me and Fernando for being such an inspiration and great motivator. Thank you all soo much for loving me and for being my pillar of comfort and motivation always and for being there the entire time throughout my course work, field work and compiling up of my final thesis.

Acknowledgments

First and foremost I would like to thank my mother Martha Shiningayamwe for raising me into a woman I am today and for guiding me throughout. Her support and unconditional love gave me the courage to work for my education and take ownership for my future. My aunty Hilja Kaholongo and her husband Mathew Kaholongo for taking care of me the past five years and for being there as my parents, I will forever be grateful.

I would like to sincerely thank all my lectures for all the help and support during my study years at the University of Namibia. I gratefully acknowledge Dr. Ansgar Wanke, Mr. Christoph Lohe and Mr. Martin Quinger for their advice, supervision and review of drafts of my thesis. I would like to further thank Mr. Martin Quinger and Mr. Christoph Lohe of the BGR (Windhoek) for offering me this interesting subject, your great assistance and support during the whole time and for giving me an internship opportunity at their office.

I am immensely grateful for the financial support of this research provided by BGR, for funding my trip and stay in Germany for my laboratory work for two weeks and the University of Namibia for the pocket money.

Declaration

I, the undersigned, hereby declare that I am aware of the concept of plagiarism and the work presented in this report is my own work obtained by researching different material with information related to the topic of study and I have therefore provided the list of references from which some information were taken. Furthermore I declare that the work presented in this thesis is my own original work and that I have not previously in its entirety or in part submitted it at any other university for a degree.

Signature:…………………

3rd December 2015

Abbreviations

General Abbreviations

BGR	Federal Institute of Geosciences and Natural Resources of Germany
CEB	Cuvelai –Etosha Basin
DWA-BGR	Groundwater Investigation of the Cuvelai-Etosha Basin of Federal Institute of Geosciences and Natural Resources of Germany (BGR) and the Department of Water Affairs and Forestry (DWAF)
DWAF	Department of Water Affairs and Forestry
MAWF	Ministry of Agriculture, Water and Forestry
KDP/ KOH-0	Discontinuous Perched Aquifer
KOH-1	Upper Ohangwena Aquifer
KOH-2	Lower Ohangwena Aquifer

Technical Abbreviations

Ma	million years
m	meter
m.b.g.l	Meter below surface
m.a.m.s.l	Meter above mean sea level
%	percent
‰	per mille
s	second

Salinity ranges	Classification	TDS [mg/l]	EC [mS/m]
	Fresh:	< 1,0000	< 150
	Brackish:	1,000 to 10,000	150 to 1,500
	Saline:	> 10,000	> 1,500
(after Plöthner et al.,1997)			

T Transmissivity in m2/day

TDS Total dissolved solids in mg/l

List of Figures

List of tables

List of appendices

Table of Content

CHAPTER 1: INTRODUCTION

1.1 General introduction

Access to safe fresh water is the main limiting factor for the economy and social development of Namibia. Surface water is mainly restricted to 4 perennial rivers at the Northern and Southern borders. Therefore groundwater in Namibia, as it is true for most arid countries, plays a vital role for the supply of wide areas. In its search for potable water, Namibia has embarked on an investigation of the groundwater resources in its part of the Cuvelai-Etosha Basin (CEB), which has total of about 160,000 km^2 in north central Namibia near the border with Angola (Lindenmaier et al., 2014).

The demand for potable water is steadily increasing as the population and economic grows. Most of the near surface groundwater in the western half of the CEB is brackish to saline (Lindenmaier et al., 2014), therefore, deeper groundwater resources needed to be investigated and tapped. The exploration of water in the CEB has been part of joint efforts by Namibian (Department of water affairs and Forestry, DWAF) and German (Federal Institute for Geosciences and Natural Resources, BGR) authorities in the Cubango Megafan, a unique palaeo-fluvial system that has supplied sediments to the north-eastern half of the CEB since at least the Miocene (Miller et al.2010; Fenner 2010; Lindenmaier and Christelis 2012) in (Lindenmaier et al., 2014) and that contains fresh water aquifers.

Namibia is an arid to semi-arid country with a low amount of precipitation and a high potential evaporation rate (Schaller, 2012).Approximately half of the Namibian population lives in the Cuvelai-Etosha Basin (CEB), that is within the central north of Namibia (Mendelsohn et al., 2000).Therefore, the whole area has a high demand on potable and domestic water. To decrease the dependency on water that is from Angola,

To decrease the dependency on water from Angola by using existing groundwater sources.

The Cubango Megafan emerges from the Angolan Highlands in the north and terminates at the north-eastern end of the Etosha Pan (Miller et al., 2010).

1.2 Location of area

The study area is located in the Ohangwena Region in the north central part of Namibia,to the south of the Angolan border.The cored borehole WW203302 is situated in Omulondo village in Epembe constituency,located about 40 km west of Okongo town.Drilling operation of this borehole commenced on the 4th December 2013 and was completed on the 20th December 2013 and was completed on the 20th December 2013.The borehole has a depth of 400 m.Average annual rainfall is indicated in Figure 2. The area lies in the hydrological Cuvelai-Etosha Basin, Vegetation is classified as Cuvelai Drainage type / North-Eastern Kalahari Wooland type vegetation (Fig. 1; MET, 2000). Populated (density of 100 people / km^2)with rural farmes, where milet (Mahangu) crop farming and livestock (cattle, goats) are the main agricultural land use.

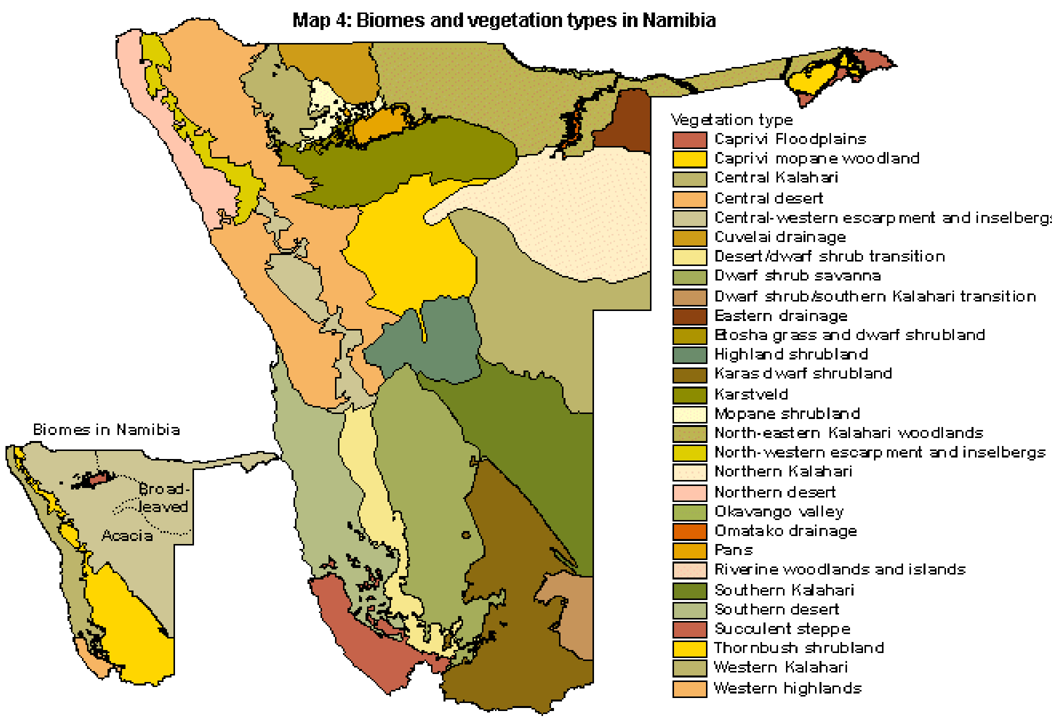

Figure 1: Biomes and Vegetation Types in Namibia (MET 2000). The Ohangwena region encompasses two Namibian biomes, the Cuvelai Drainage and the North-Eastern Kalahari Woodlands.

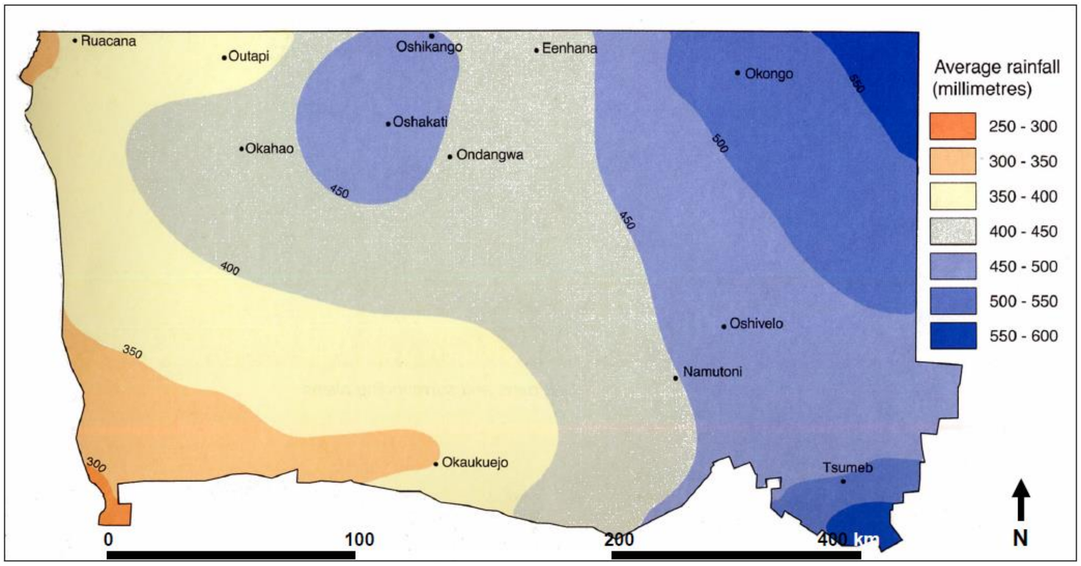

Figure 2: Average annual rainfall across north central Namibia (BIWAC, 2006 after Mendelsohn et al., 2000).

1.3 Statement of the problem

Various perched aquifers and two deep aquifers have been discovered in the Ohangwena region. The presence of a third aquifer is still to be confirmed. The hydraulic parameters of the according aquifer, aquitard, and aquiclude intervals haven't been established yet. However, any groundwater flow model, including sustainable yield assessments, requires the knowledge of the essential hydraulic parameters, namely permeability and effective porosity. Therefore the determination of those parameters in their stratigraphic context is central for any further groundwater investigations in the Ohangwena region.

1.4 Objectives

- Produce a core documentation/core log on principal lithological characteristics from 0-150 m depth of the core

- Establish the hydraulic parameters (porosity and hydraulic head/permeability) of aquifers and aquicludes/aquitards in the samples taken

1.5 Significance of study

Hydraulical parameters are central in understanding the hydrogeology of the Ohangwena Region. Aspects such as groundwater flow, sustainable abstraction rates, and groundwater vulnerability are largely a function of hydraulic parameters. Therefore; this study will bring a clear understanding to these aspects and will help assist in any further studies on the Ohangwena aquifers should there be any.

1.6 Limitations of study

- The study is based on one borehole only
- Most data will only be available at the end of the semester
- It’s not a comprehensive regional study as it’ s a scope of a BSc project

CHAPTER 2: LITERATURE REVIEW

2.1 Geological Overview

The study area is situated in the intra-continental Owambo basin was formed during the post Cretaceous tectonic development of southern Africa (Momper, 1982).The Owambo originated from the breakup of a super-continent named Rodinia and it is located on the Congo Craton between 14◦E to 18◦E and between the northern border of Namibia to 19◦15'S (Miller, 1997). It extends northwards into southern Angola and possibly continues into western Zambia (Walzer, 2009).

Furthermore, the Owambo basin is floored by mid-Proterozoic crustal rocks of the Congo Craton and contains about 8000 m of sedimentary rocks of the Nosib, Otavi and Mulden Groups of the late-Proterozoic Damara Sequence (Miller, 1997). In addition, about 360 m of Karoo strata are overlain by a blanket of semi-consolidated to unconsolidated Cretaceous to Recent Kalahari sequence sediments of approximately 600 m thickness (Walzer, 2009). The geological information on the Owambo basin was generally achieved from outcrops along its margins, interpretation of aeromagnetic, seismic and gravity surveys as well as thinly distributed wells (Miller, 2008c). The Ohangwena Region is situated in the intra-continental Owambo Basin, which was formed during the post-cretaceous tectonic development of southern Africa (Momper, 1982). Overall, the geology of the Owambo basin contains rocks and sediments of the Damara Sequence, the Karoo Sequence and the youngest Kalahari Sequence which all overlie Precambrian basement rocks of the Okongo Craton.

The sediments found in most drilling material in the region belong to the Kalahari Sequence. These sediments resulted from the erosion of mountains in Central Angola and it is believed that a considerable amount of the Kalahari sediments must have been reworked. According to Mendelsohn (2000), cycles of climate with wet and dry periods followed each other and rivers that drained into the basin deposited the sediments that formed the Ombalantu, Beiseb, Olukonda and Andoni Formations of the Kalahari Sequence.

2.2 Damara Sequence

The Damara Sequence evolved on a rifting margin, with sedimentation starting at 900 Ma with terrestrial-fluvial sandstone of the Nosib Group. This was subsequently followed at 730 to 700 Ma ago with carbonates of the Otavi Group. These carbonates are dominantly dolomite with some limestone and shale deposited in a marine platform environment .At contacts to low permeable rocks and in fault zones the carbonates became locally karstified.Finally between 650 and 600 Ma deposition of erosion products of uplift produced the Mulden Group rocks ranging from sandstone, siltstone and shale to carbonate (Miller,2010). During and after the deposition of the Damara Sequence, a period of tectonic activity resulted in faulting and folding, followed by a period of erosion.

2.3 Karoo Sequence

In the CEB Karoo Sequence rocks do not crop out at surface .The evidence from studies of previous boreholes suggests that the Karoo consists of fluvio-glacial deposits of the Dwyka Group, mainly tillite, sandstone and shale (Miller, 2008c).Fluviatile reworking of the Dwyka Group and a post-glacial environment led to the deposition of shale, sandstone and carbonate of the Prince Albert Formation.

The Etjo Formation which may reach a thickness of 140 m is represented by mainly red sandstone deposited through the action of wind during arid conditions in Jurassic times and is intersected by several boreholes in the surrounding of Oshivelo (Bittner et al.,2006).

The basalt of the Kalkrand Formation intruded in late Karoo times (170 Ma).Intrusive dykes, inferred from aeromagnetic anomalies, extend throughout the area north of Tsumeb and are considered to be coexisting with basaltic flows. A north-east trending fault (at the southern margin of the Etosha Pan and NNE trending fault (east of Oshivelo) are supposed to truncate the Karoo sediments (Lindenmaier et al ,2014).The S-N trending Oniimwandi Dyke Swarm is believed to be intruded during late Karoo times aswell.

2.4 Kalahari Sequence

Studies on the Kalahari Sequence have been carried out by various authors, such as Miller (2008c) and Bittner (2006).

For the past 70 years the Owambo basin has been filling up with sand, silt and clay, that was eroded from higher grounds surrounding the area (Walzer, 2009).Cycles of climate change with wet and dry periods followed each other (Mendelsohn et al, 2000). Rivers that drained into the Owambo basin, brought sediments with, that are today known as deposits called Ombalantu ,Beisep , Olukonda and Andoni formations (Walzer,2009).The Ombalantu deposits represents the base of the four formations, while the Andoni represents the top. These four formations form the youngest unit of the Owambo basin the Kalahari sequence. The following lithological and stratigraphical descriptions of the Kalahari formations are based on the work of Miller (1997, 2008c) and mainly consider the sediments and their distribution within the Cuvelai-Etosha basin as part of the larger Owambo basin.

Much of the sediment in the Owambo basin is largely unconsolidated or only partially consolidated and appears to have been deposited by the sand-dominated Cubango megafan in the east and by the much smaller, mud dominated Kunene fan in the west (Miller, 2008c).The exact timing when the Kalahari deposition began and what constitutes the base of the Kalahari in the Kalahari basin is not well defined. In Namibia, Botswana and South Africa, the base of the Kalahari Group is taken as the first unconsolidated sediments that overlie hard basement rocks, commonly of the Karoo Supergroup (Miller, 2008c).

Table 1: Stratigraphy of the Kalahari Sequence (Miller, 1997). Note that there is uncertainty about the exact location of the Cretaceous-Tertiary boundary.

Era	Sequence	Formation	Lithology	Max thickness (m)
Recent to Tertiary	Kalahari Sequence	Andoni	White sand, light green clayey sand, green clay	550
		Olukonda	Reddish brown, poorly sorted sand	152
Cretaceous		Beisep	Red sand and clay	50
		Ombalantu	Red semi-consolidated clay	80

Ombalantu Formation - A basal, red, fine grained, semi consolidated but friable formation with variably silicified mudstones but almost entirely consisting of clay. It does not crop out, has a broad elongate distribution extending from the southeast to the north- west of the basin and reaches a maximum thickness of 80 m (Walzer, 2009). Gypsum and Gypsum crystals occur in the upper part of the formation. Miller (2008c) evaluates its deposition to be mainly of the accumulation of fine clastics in a shallow, low energetic, deltaic environment. A restricted continental basin with a significant and sufficient amount of evaporation was required to lead to the appearance of gypsum.

Beisep Formation - A gravel deposit which is widespread, generally reddish in colour it represents a period of rapid and extensive input of material from the basin margins (Walzer, 2006).With a maximum thickness of 50 m it is the thinnest of the Kalahari Formations. It consists of well-rounded sand and clay stone clasts which are set in a matrix of fine to medium grained, argillaceous, and calcareous to dolomitic sandstone (Miller, 2008c).

Olukonda Formation - A friable, poorly consolidated, reddish brown, poorly sorted massive sand and sandstone formation with a limited distribution but a broad elongate sub outcrop similar to the Ombalantu Formation. It contains a few thin gritty and pebbly layers and is up to 152 m thick (Miller, 2008c).

Andoni Formation - It occurs throughout the Owambo basin as a cover to all underlying units and consists of interbedded white medium grained sand, light greenish clayey sand and green clay (Miller, 2008c). In zones, the predominantly sand varies between 10 and 200 m and shows an unconsolidated, slightly pyritic or hematitic condition. The top part of the section contains numerous irregular shaped dolocrete and calcrete nodules which are embedded in polished, angular to sub rounded grains of quartz which in turn make up to 90 % of the sand (Miller, 2008c). Sorting improves upwards in the sequence. The appearing of clay layers within this formation varies in thickness between a few centimetres and 150 m (Ombalantu borehole in Miller (2008c)). They are often silty and/or sandy.

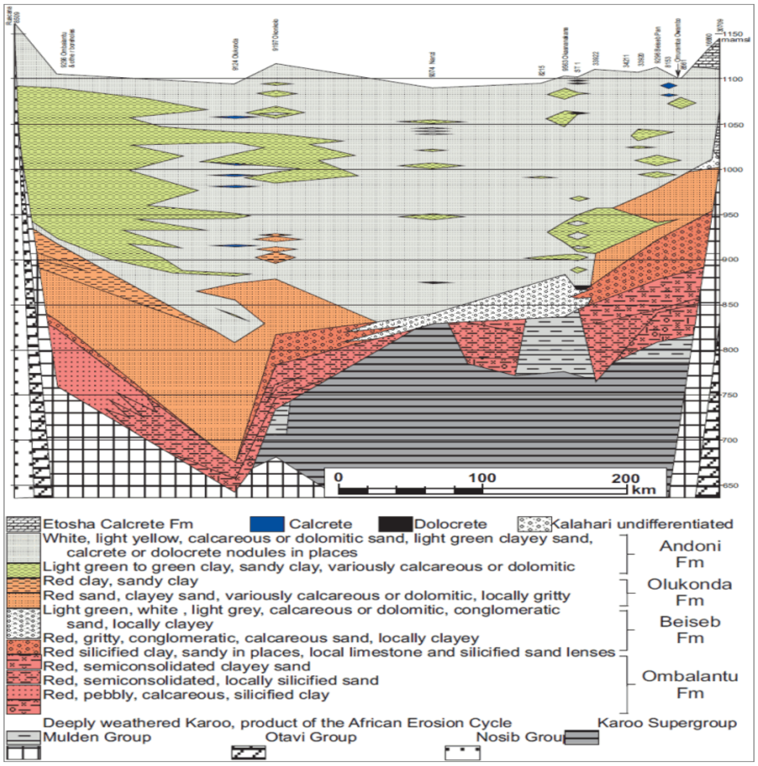

Figure 3: Stratigraphy of the Owambo basin formation (Miller, 2008c).

2.5 Hydrogeological setting

The Ohangwena Kalahari Aquifer System is one of the six aquifer systems in the CEB. It is a multi-layered, continuous porous aquifer system of the eastern Ohangwena and northern Oshikoto Regions with an estimated groundwater flow from Angola towards the Etosha Pan (Schaller, 2012). It represents the main fresh water source of the Niipele Sub-basin (one of four sub-basins in CEB) of which 300 000 m³/year are used for water supply to most of the scattered villages. The KOH consists of shallow perched aquifer lenses (KOH 0), an upper Ohangwena Kalahari I Aquifer (KOH 1) and a lower Ohangwena Kalahari II Aquifer (KOH 2) separated by an aquiclude/aquitard.

KOH 1 is situated at a depth between 60 and 160 m.b.g.l. and comprises greenish, semi-consolidated sandstone of the Andoni Formation (BIWAC, 2006). KOH 1 is limited by administrative borders towards the north (Angolan border) and east (border of the CEB) whereas the southern and western expansion is determined by its hydrochemical conditions (Schaller, 2012). The recharge area is assumed to be within the highlands of south-eastern Angola. KOH 1 represents a major fresh water source within the Ohangwena region. Due to mixing processes with saline groundwater from the adjacent aquifers, water becomes brackish to saline towards the southwest and is therefore not suitable for drinking water purposes (Schaller, 2012).

KOH-1 it is an important aquifer for dispersed exploitation by means of relatively shallow boreholes with a variety of pump tests (Lindenmaier et al.,2014).The Rural Water Supply authority of the Ministry of Agriculture, Water and Forestry of Namibia (RWS) drills and maintains most of these borehores.During droughts,KOH 1 is used as a water supply additional to that of the KOH-0.Yield and quality of water of the KOH-1 is low and very variable ,therefore, it is primarily used for livestock (Lindenmaier et al.,2014)

The deeper- seated KOH 2 is a fresh water aquifer, situated within the Olukonda Formation at a depth between 130 and 380 mbgl and comprises mainly red sandstone and clay. As with KOH 1, the recharge area is assumed to be in Angola. The expansion of KOH 2 towards the southwest is determined by its hydrochemical conditions (Lindenmaier et al., 2014). The approximate boundary runs along the line Oshikango-Okankolo, suggested by measurements of saline boreholes west of Oshikango and two saline artesian wells east of Ondangwa. For statements on the continuation of the aquifer in southern Angola hydrochemical data from this region is necessary.

Indications of the deep-seated freshwater aquifer (KOH2), were first described by Bittner (1998),who drilled a deep borehole (WW37070) for DWAF that reached freshwater at a depth of 190 m (Lindenmaier,2014).

Towards the east it is assumed that KOH 2 merges into KOH 1. The exact course of the border is unknown as yet. However, according to BIWAC (2006) two separated aquifers have been discovered in the Okongo area.

2.5.1 The Cuvelai – Etosha Basin

The Cuvelai-Etosha Basin (CEB) is a large endorheic hydrological system in the south-west of Africa extending from the southern Angolan Highlands into north-central Namibia (Figure1a)

(Lindenmaier et al.,2014)).It is flanked by catchments of the Kunene and the Okavango in the north. The folded and karsted platform carbonates of the Neoproterozoic Otavi Group form a topographically elevated margin to the south and west of the basin (Figure 1b) (Lindenmaier et al., 2014).The crest of the Cubango Megafan forms the approximate eastern limit of the CEB.

The Cuvelai-Etosha represents a huge aquifer system with sediments of the Kalahari formation (sand,sandstone,silt,clay,calcrete) with thickness of several 100 meters covering the underlaying bedrock (Miller,2008c).Groundwater in the Cuvelai-Etosha Basin is found in a complex system of the stratified, partly braded aquifers containing fresh and/or saline water. The spatial distribution of fresh and saline water has yet been established and the distribution of the depths and potential yields of the different layers is not yet known.

Annual rainfall is between 400 and 500 mm within the CEB (Mendelsohn et al., 2000) but is up to 1,100 mm at its northern tip in the Angolan highlands (Verissimo, 2005) in Lindenmaier et al (2014), the main headwater catchment of the Kunene, Cuvelai and Okavango River systems. In contrast, annual potential evaporation is estimated at about 2400 mm (Mendelsohn et al., 2000) in Lindenmaier et al (2014).Current climate is highly seasonal with a rainy season in December to March and a dry season in April to November (Lindenmaier et al. 2014).The amount and distribution of rain is highly variable, which is also true in regards to long term fluctuation.

All groundwater within the Cuvelai – Etosha Basin (CEB) flows towards the Etosha Pan, which is the base level of the groundwater flow system due to the structure of the basin and because the pan is the deepest point (Bittner, 2006). Three main groundwater flow systems can be determined within the CEB due to its basic topography (Bittner, 2006).

1. Groundwater that is recharged in the fractured dolomites of the Otavi Mountain Land at the southern and western rim of the basin. It flows northwards and feeds the aquifer system of the Karoo and Kalahari sequences (Bittner, 2006).The major part of this water evaporates rapidly as it discharges through springs along the southern margin of the Etosha pan.

2. A deep seated, multi-layered Kalahari Aquifer System which flows from Angola in southern direction towards the Etosha Pan and the Okavango River.

3. A shallow Kalahari Aquifer in the central part of the CEB which superimposes both previously described groundwater flow systems (Bittner, 2006). It mainly consists of saline water and originates from regular floods, respectively from the Efundjas whose runoff is determined by the ephemeral stream, respectively Iishana.

2.5.2 The Ohangwena Aquifers

The Ohangwena Aquifer (KOH) is a multi-layered porous aquifer, occurring in the Cubango Megafan; it was discovered in the east of Ohangwena region (Lindenmaier, 2014). The aquifer lies in the Iishana and Nipele subbasin and the groundwater is estimated to flow southwards in the direction of the Etosha Pan (Walzer, 2009). The KOH consists of two main aquifers, the upper KOH 1 aquifer and the deep seated freshwater aquifer KOH 2 (figure 4). It is assumed that the upper KOH 1 aquifer is separated by an aquiclude or aquitard to the deep seated aquifer KOH 2. KOH 1 has been intersected between Eenhana and Okongo at depths between 60 and 160 m and represents a major water source within the Ohangwena region (Bittner, 2006). It consists of the light greenish clayey sand of the Andoni Formation and appears in terms of fresh water close to the Angolan border. The KOH 1 is recharged by lateral through flow from a proposed unconfined Kalahari aquifer in the southern Angola. The aquifer becomes brackish to saline towards the south with a distance of a few kilometres and it is therefore not developed for drinking water purposes (Walzer, 2009).

The deep seated fresh water aquifer KOH 2 was encountered in the Nipele-subbasin and it's assumed to have a continuous and regional extend. Due to its great depth from 130 m to 380 m it is situated partly within the Olukonda Formation and has not been explored precisely (Walzer, 2009). Like KOH 1 the recharge area is assumed to be in southern Angola. The water quality is fresh for the east and north of Eenhana but becomes more saline towards the south-west where it is still regarded as water of good quality according to the Namibian Drinking Water Classification System (based on values of electric conductivity).

The Ohangwena Aquifer (KOH) also consists of a third aquifer, the uppermost discontinuous perched aquifer (KDP of Bittner and Kleczar (2006) in Lindenmaier et al (2014), which occurs in the aeolian sheets sands, is found throughout the CEB and is named KOH-0.The Ohangwena

Aquifer KOH-0 is an important source for potable water for the local population but yields are limited and little is known about the aquifer, therefore, it is not a target for large-scale exploitation. Its spatial and even temporal distribution is closely related to the rainfall as it is fed by direct infiltration.

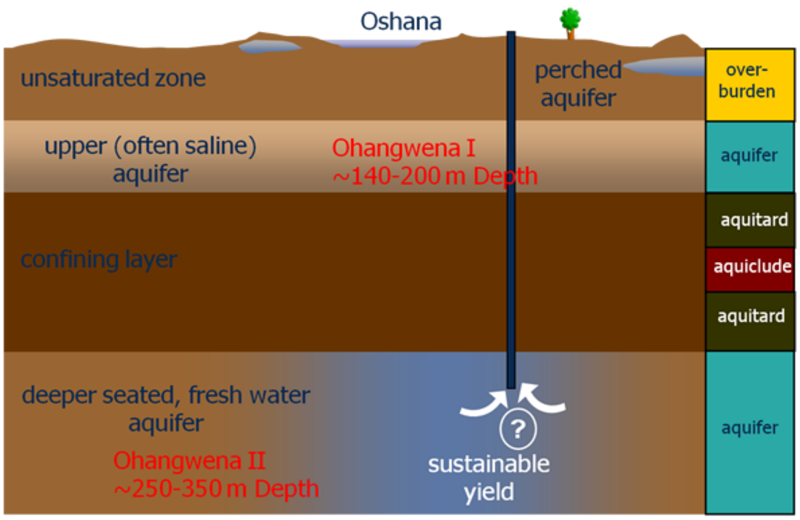

Figure 4: The Ohangwena Aquifers.

2.5.3 Hydraulic Parameters and its measurements

The determination and estimation of hydraulic parameters such as permeability and porosity that effects the rention and movement of water and dissolved substances through soils, plays a major role in understanding water management, groundwater flow modelling, including sustainable yield assessments and soil engineering. Therefore the determination of these parameters is one the major requirements in understanding the Ohangwena aquifers.

Hydraulic conductivity of soils (a term used to describe permeability in soils) is measured using a mathematical law that is popularly known as Darcy's law, which is a law that describes the flow of water through a porous medium. As shown in figure 5, a tube is filled with a porous medium and it is then vertically tilted to an angle with water that is introduced into the top of the tube. According to the equation the volumetric rate ''Q'' at which water entering the tube at the top is equal to the rate at which the water leaves the tube at the bottom Taking into consideration the difference in water heads "Δh" at two points, monitored through the aid of two vertical pipes installed at distance “Δs” at the tube (figure 5), Darcy expressed the volumetric flow through the tube as:

$Q\ (m^3s^{-1}) = q\ (ms^{-1}) * A\ (m^2)$

Where: Q = the volumetric flow rate [L3/T]

A = the area perpendicular to the flow [L2]

q = the specific discharge through the tube [L/T] which he defined as:

$q=-k\Delta\ (\Delta h/\Delta s)$

Where: K = a constant known as the hydraulic conductivity of the porous medium [L/T].

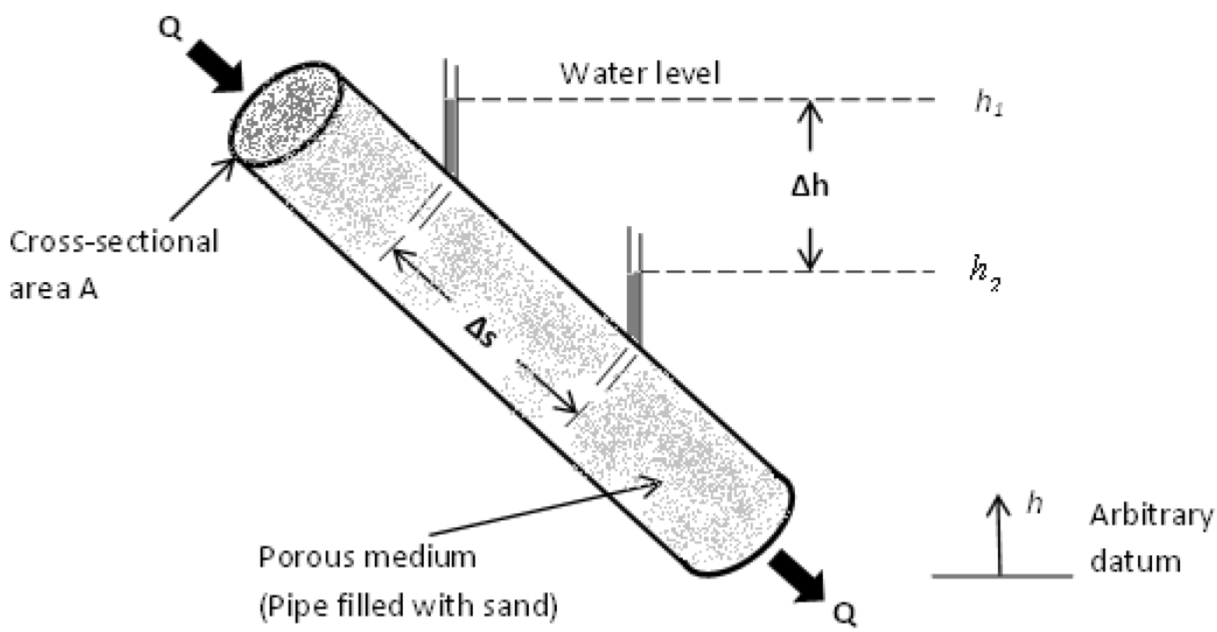

Figure 5: Experimental apparatus used to derive Darcy's Law (Walzer, 2009).

Though Darcy’s empirical description of flow through a porous medium is a generally accepted equation especially in the fields of hydrology and groundwater engineering, it has both upper and lower limit of application (Akanegbu, 2013). For instance, it does not hold at very high fluid velocities, and there are some questions about whether or not it is an accurate description of fluid flow for very low head gradients, especially in materials of low permeability (Akanegbu, 2013) after (Deming, 2002). Darcy's law is based on the assumption that soils were merely a bundle of straight and smooth tubes, with each having a uniform radius. But in reality, soil pores are not uniform, smooth and cylindrical tubes, but are irregular in shape, tortuous and intricately interconnected (Akanegbu, 2013) after (Hillel 1998). Water flow through soil pores is dependent on both the properties of the medium and the properties of the fluid flowing through the medium. It depends on the pore geometry of the soil as well as the density and viscosity of the fluid.

2.5.4 Soil properties affecting hydraulic conductivity and porosity

Hydraulic conductivity is mainly controlled by the arrangement of soil particles within a soil. The pore geometry and continuity within a soil changes depending on the direction of measurement. The vertical component of K is different from the horizontal component in most cases. One measurable property of soil pore geometry that is most influential in soils hydraulic conductivity is porosity which is given by:

$n=Vv/VT*100$

Where: n = the porosity of the soil sample (%)

Vv = the volume of voids in the soil sample (m^3)

VT = the total volume of the soil sample (m^3)

The porosity of soil decreases with depth and is best expressed using void ration which is given by:

$E=Vv/Vs$

Where: Vs =volume of solids (m^3)

The preference of void ratio to porosity is due to the fact that any change in the volume of a soil mass is a direct consequence of a similar change in the volume of voids while the volume of solids remain intact. Porosity varies inversely with the soil dry bulk density while the relationship between void ratio and porosity is given by the expression:

$n=e/ (1+e)$

Effective porosity is the ratio of the volume of the pores which are interconnected in the rock to the total volume of the rock while, the total porosity is the ratio of the entire pore space in a rock to its bulk volume.

CHAPTER 3: RESEARCH METHODOLOGY

In order to meet the objectives of the study, several techniques/methods were employed such as sampling, core logging, and sample preparation for analysis, and laboratory work. Literature study was conducted to understand the background of the laboratory tests such as the falling head method for the permeability test, porosity test and texture analysis with sieving, and sedimentation technique.

Desktop studies have been made for all aspects of the research subject. Journals, textbooks and technical reports were consulted to understand the Ohangwena Aquifers. Reports of previously drilled boreholes in the Ohangwena Region where the Ohangwena Aquifers were encountered had been viewed and relevant information extracted. Virtually no previous work has been carried out on the Ohangwena Aquifers in the study borehole, especially information regarding hydraulic parameters and the main lithological properties have been lacking. Literature study aimed to understand the nature of sediments to be found in the core WW203302.

3.2 Field Work

3.2.1 Log and Stratigraphy of borehole WW203302

The core was successfully logged the first week of the field. Logging went till the depth of 250 m; however, the project is focused until the depth of 150m. The basic information that was included in the logging was the stratigraphy to be documented in a core-litholog. The main aspects are principal lithology that includes texture, gross composition, colour, compaction, stratification, and cementation of strata.

The information derived from the geological logging of the core WW203302 was the type of rock it is, the colour, the grain size and the amount of calcrete and dolocrete in the core.

3.3 Laboratory Work

Various laboratory methods of estimating hydraulic conductivities of soil samples were reviewed by Klute and Dirksen (1986, 687-734) in (Akanegbu, 2013). According to them, the laboratory methods are divided into two categories: methods that are applicable to saturated soil and methods that are applicable to unsaturated soils, but given the nature of this study, only the method applicable to saturated soil is discussed and used.

The laboratory method used for this project is the falling head permeameter method.

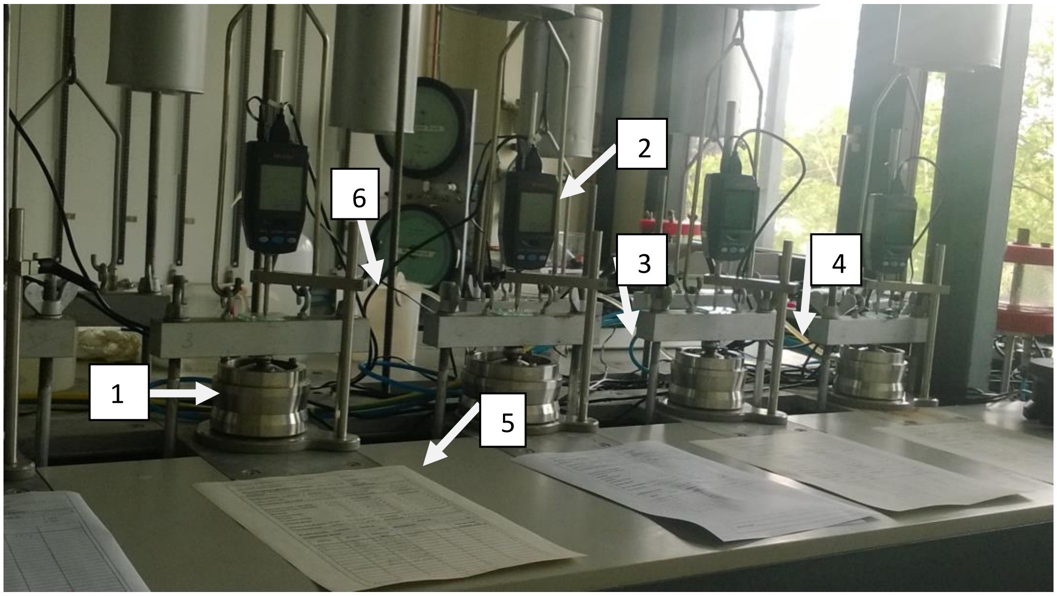

Figure 6: Falling head permeameter apparatus. (1) = Core Cell, (2) =Timer, (3) =Inlet, (4) =Outlet, (5) =Recording Sheet, (6) =Beaker.

3.3.1 Falling head permeameter method

The falling head method operates with the principles of Darcy equation as in the constant head method except that in its case, the hydraulic gradient changes with time unlike in the constant head method where the hydraulic gradient is constant. This system is mainly applicable to soils with low hydraulic conductivity where accurate measurement of discharge using a constant head permeameter is difficult. A simple illustration of the falling head permeameter principle is shown in figure (6).

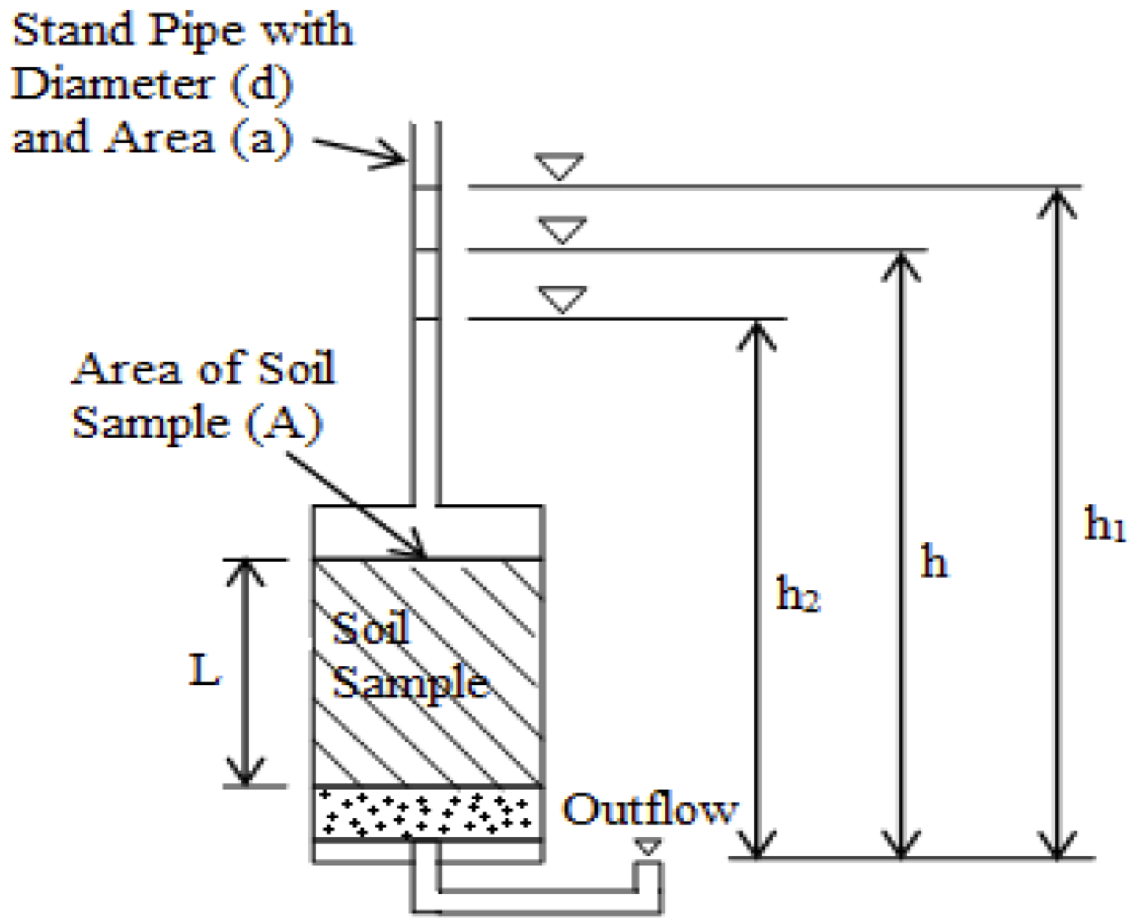

Figure 7: Illustration of the operation of falling head permeameter (Ranjan and Rao 2000, p141 in Akanegbu 2013).

A cylinder with a porous plate at the bottom is placed with an undisturbed soil sample, above the sample is a standpipe connected above it as shown in figure (7) and figure (8). The elevation difference "dh" in the water level in the standpipe at any given time "dt" is noted by filling the standpipe with de-aired water and at the same time allowing the water to flow through the soil sample. Since the volume of the water that is passing through the sample in time "dt" is known, the hydraulic conductivity of the sample being tested is calculated using the mathematical expressions:

-a (dh/dt) =K (h/k) A

The left side of the equation (-a (dg/dt)) represents flow in unit time through the sample which is (a*velocity of fall) and the negative sign of the results shows that the head decreases with time, while the right hand side of the equation (K (h/k)A) represents Darcy flow q which is given by (K(h/l)A).

Rearranging and integrating the above equation, the hydraulic conductivity is thus given as:

K= (al/ (A (t2-t1)) $\log_e$ (h1/h2)

Where a = the cross-sectional area of the standpipe [L2]

L = the length of the soil sample [L]

A = the cross-sectional area of the soil sample [L2]

h = the hydraulic head difference across the sample at time t [L]

h1 = the initial hydraulic head [L]

h2 = the final hydraulic head [L]

t1 = the initial time at h1 [T]

t2 = the final time at h2 [T]

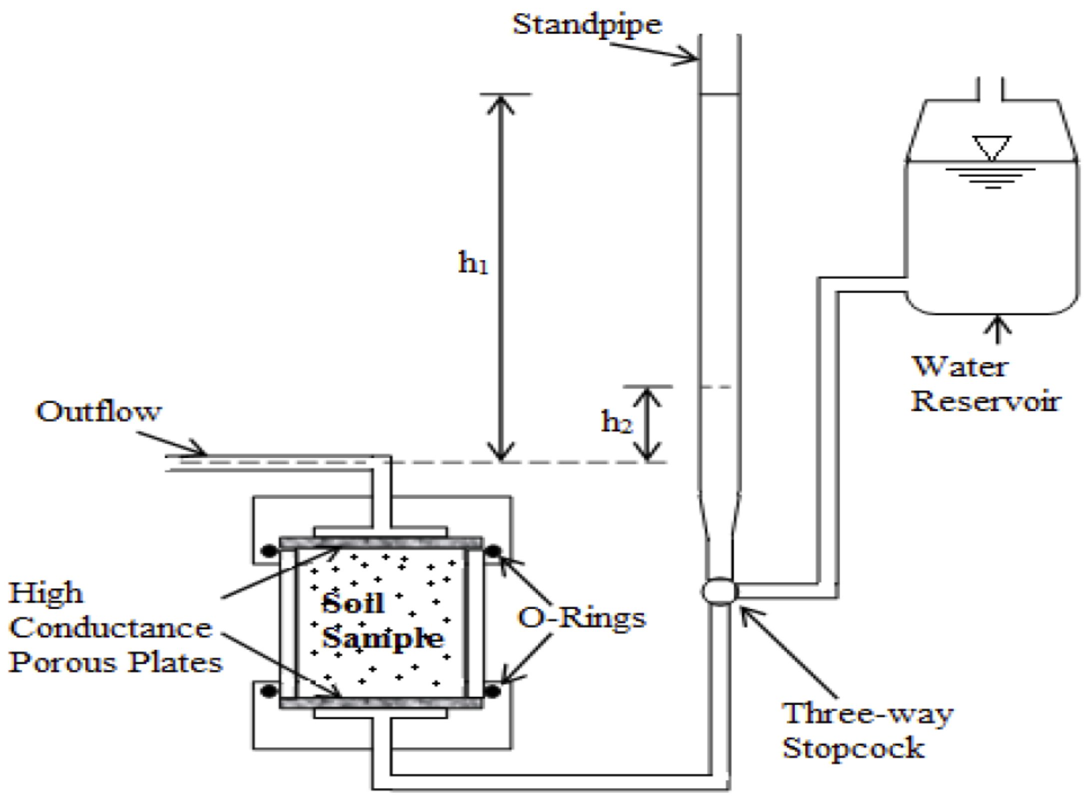

Figure 8: A typical setup of apparatus for measuring hydraulic conductivity by falling head permeameter method Klute and Dirksen, 1986, p701 in Akanegbu 2013).

3.3.2 Sample correction and preparation

Soil samples were collected from the core. A total of 20 samples were taken, at an interval of 10 m each from the top of the core till 150 m depth. The samples were then taken up the lab were they got prepared for the permeability test (falling head method). The samples were cut to fit well in the sample holder ring for the falling head method test. Some samples were hard; therefore, a drill tool was used to fit the samples in the ring for the test to begin. Samples that were waiting for the test were sealed well in plastic bags to prevent them from getting dry or wet. The sealing of the sample bags was made by using an electronic sealing machine.

(a) (b)


Figure 9: (a) Preparation of samples for the hydraulic head; fitting of the sample into the sample holder ring. (b) Preparation of the hard samples (Photo taken by Joseph Reginalda, 2015)

(c) (d)
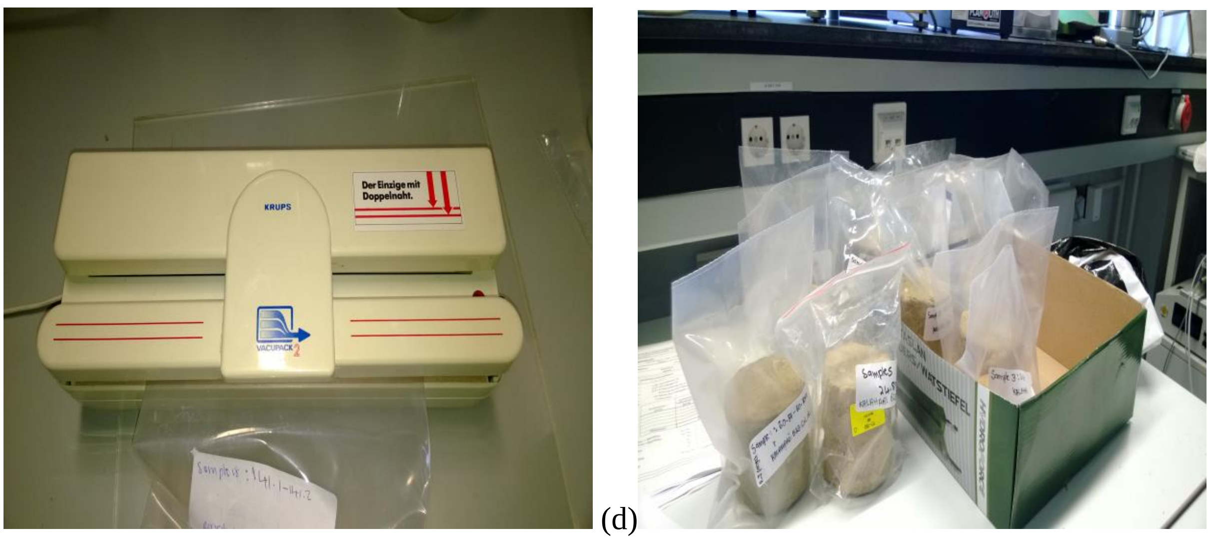

Figure 10: (c) A sealing machine used to seal the sample bags. (d) Samples in the sample bags after sealing (Photo taken by Reginalda Joseph, 2015)

3.3.3 Hydraulic Parameters

Measurements of the Texture, Porosity, permeability, and hydraulic conductivity were analysed, studied and calculated for the core in the Hannover BGR lab in Germany. This was done by evaluating the core drilling and carrying out permeability tests.

The falling head permeameter method was adopted for the laboratory test. The test was conducted on 20 samples with different depths ranging from 9.7 m to 150 m depth. The samples were fit into core rings (figure 11) with a surface area ranging from 0.001993m^2 and 0.001995m^2.

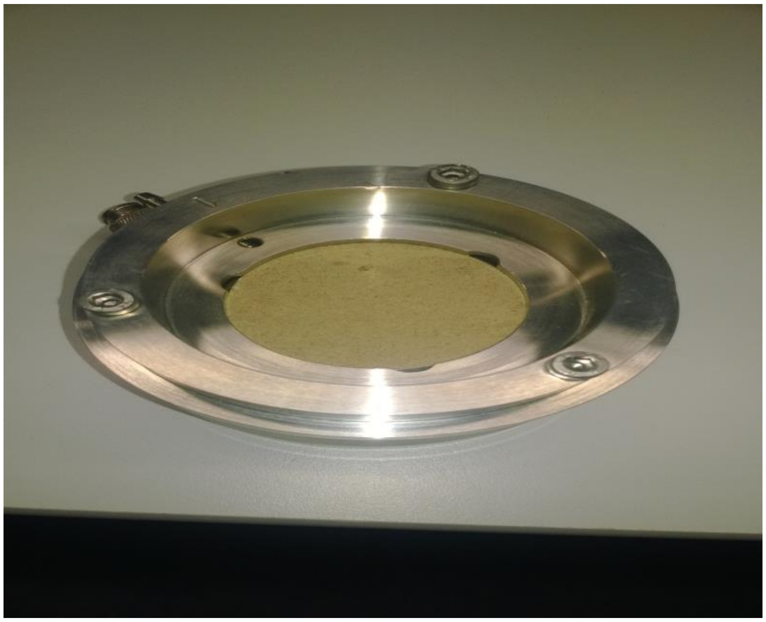

Figure 11: Sample fitting into the sample ring for the permeability test (Photo taken by Reginalda 2015).

3.3.4 Determination of the effective Porosity

Porosity is the volume of void space in a geologic material. The amount of water available within a rock or sediment when saturated is determined by the specific yield as the empty spaces within these sediments and rocks are usually occupied by groundwater. Therefore, porosity can be defined as the specific yield minus the specific retention. Effective porosity is important for hydrogeological studies as it relates to hydraulic conductivity and storativity.

18 samples from different depths until 150 m were used to test for the porosity. The following procedures and mathematical expressions were used:

1. Drying the sample at 80°C to remove all pore water
2. Weighing the sample (Dry weight) after 24 hours of drying
3. 3.'Bathing' the sample in water and extract the air in the pores with a vacuum
4. Release the vacuum (pores fill with ethanol)
5. Weighing water saturated sample: n_1

The effective pore volume is then calculated with the equation:

$$V_p = (n_1 - n_0)/D\ (\text{water})$$

V_p= effective pore volume

N_1=Weight of sample saturated with ethanol

N_0=Weight of dry sample

$D_{(water)}$ =specific density of water

3.3.5 Texture analysis (Grain Size Measurement)

The grain size analysis was carried out by a mechanical analysis: a total 9 sieves were used to determine the grain size distribution of the same sediment samples that were previously used for the permeameter tests. The sieves were chosen according to the expected grain-size spectrum, and to approximately match the grain-size subdivisions of the sand and silt subdivisions of the Udden-Wentwoth grain size scale (figure 14). A stack of the sieves with the following mesh widths was assembled (stacking order upwards): 40-63 µm, 63-100 µm, 100-150 µm, 150-200 µm, 200-400 µm, 400-500 µm and 500-800 µm. Figure 13 shows a sieve assembly on a Retsch AS 200 sieve shaker.

The following procedure was carried out:

- Drying samples in a drying oven (figure 12) at 80° C for 24 hours
- Gentle crushing of semi-consolidated samples using a mortar and pestle
- Weighing bulk samples
- Sieving
- Weighing each grain-size interval to an accuracy of 0.01 g
- Calculation and drawing of a cumulative frequency curve

Sieving loss was estimated by summing up the weights of all grain-size fractions and comparing them with initial dry sample weight. Sieving losses were negligible for all samples.

Figure 12: Drying Oven (Binder) for drying samples before sieving. (Photo taken by Reginalda, 2015)

Figure 13: Sieves used for grain size analysis .The Retsch AS 200 sieve shake was used to facilitate the movement of sediment through the sieves (Photo taken by Reginalda, 2015).

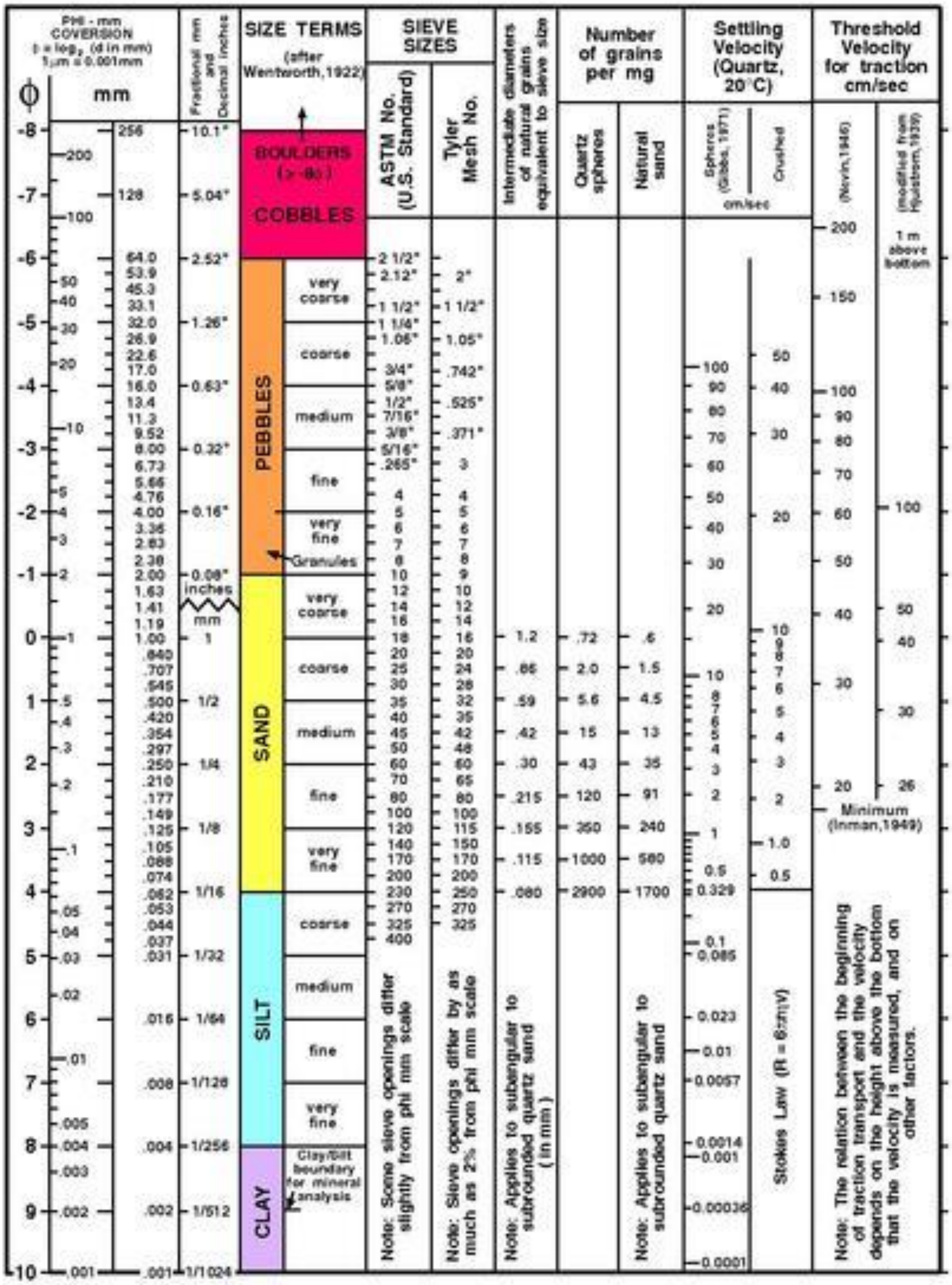

Figure 14: Udden-Wentworth scale grain size chart from United States Geological Survey Open-File Report 200-1195.

CHAPTER 4: RESULTS

4.1 Introduction

This chapter is a presentation of the outcomes of the project. It includes the results obtained in the field by core logging and in the laboratory by the falling head method (hydraulic conductivity test), and the grain size analysis with the Retsch sieving machine. The chapter includes raw data, result tables and the litholog column of the first 200 m of the 400 m core.

For clarity, the results obtained from the laboratory and field logging is presented into three sub-heading dealing with: log and stratigraphic column of the core, hydraulic parameters (hydraulic conductivity and porosity), and texture analysis. Studying hydraulic conductivity of any type of soil cannot be effectively carried out without understanding the soil geometric properties which has a major effect on water conductance through the soil, as the water movement in soils is governed mainly by soil pore geometric properties.

Therefore, to be able to achieve the main objective of the study which is determining hydraulic parameters of the borehole WW203302, it's important that a base for a comparison between the soil pore geometric properties and the hydraulic conductivities obtained is build.

4.2 Log and Stratigraphy column

The core was successfully logged and a litholog was produced. The log indicates clearly that the core is composed of very light green medium to very fine sand, with minor silt and clay interchanging with different depths. At depth (79.8 m – 108.8 m) where KOH-1 is located, the sand is more medium to fine grained with very minor silt and clay, while at depths (8.7m- 69.7 m) and (118.8m – 157 m) where aquicludes are located the sand is more fine to very fine grained with higher silt and clay contents. Sands tend to be slightly coarser with minor sand-clay contents at the depth interval from 79.8 m to 108.8 m, coinciding with the location of KOH-1. The core is composed of semi-consolidated material sandy material with various amounts of calcareous and dolocrete nodules. Bioturbation of various degrees is very common, while undisturbed stratification, mostly lamination has been observed rarely.

The litholog below (figure 14 (a) and figure 14 (b) give a summary of lithological characteristics. More details are given in the tabular lithology of appendix 2.

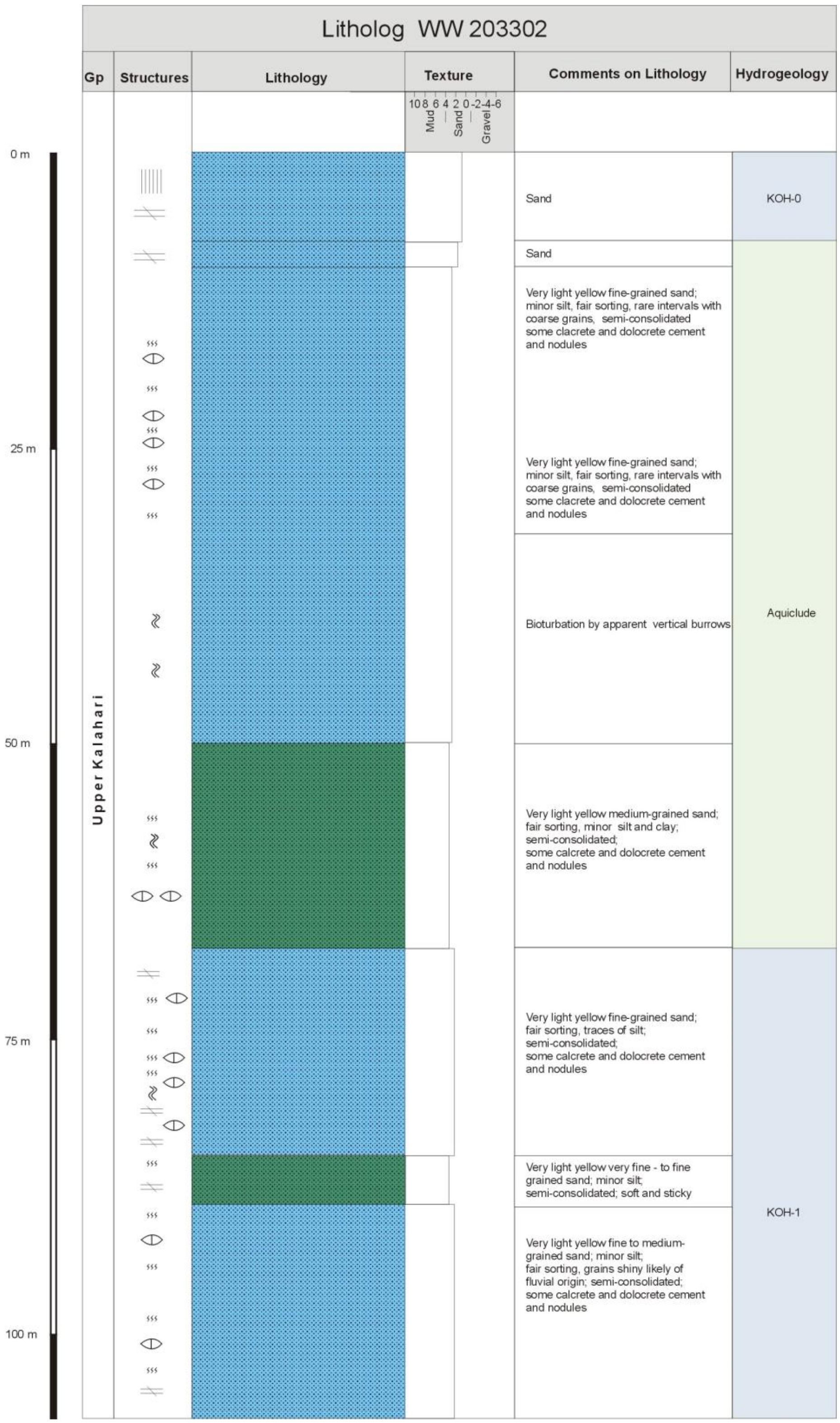

Figure 15 (a): Summarized litholog of borehole WW 203302.

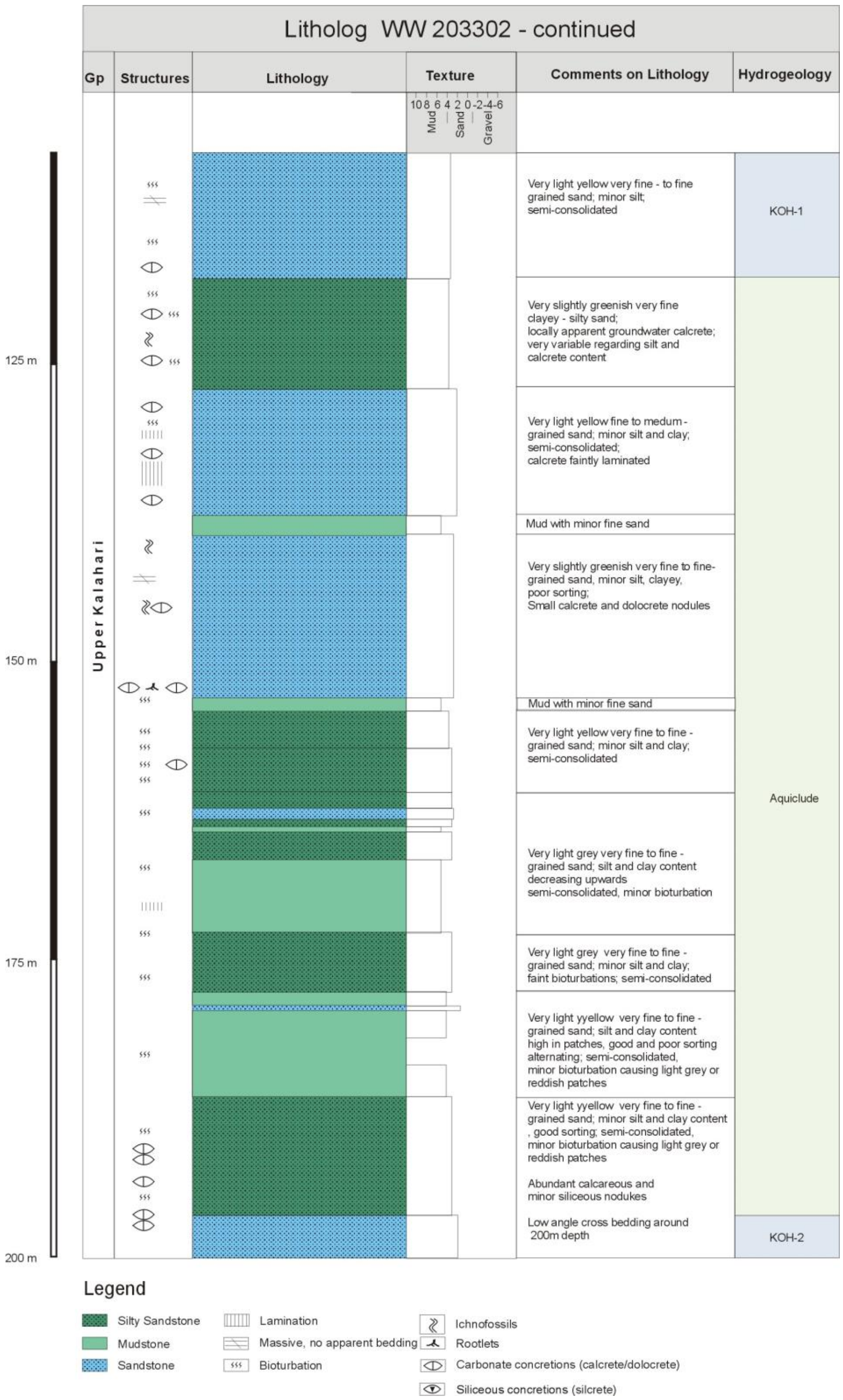

Figure 15(b): Summarized litholog of borehole WW203302.

4.3 Hydraulic conductivity

Hydraulic conductivity has been determined directly with a falling head permeameter. In addition the sediment grain-size sorting obtained from the sieving analysis.

4.3.1 Falling Head Permeameter Results

Hydraulic conductivities were obtained using the falling head method. 20 samples were taken for the experiment as mentioned in the methodology chapter; however, only 18 samples were used for the experiment. The results are given in table 3.

Table 2: Hydraulic conductivity to depth. Hydraulic conductivities have been obtained with the falling head permeameter method.

Sample no.	Sample depth (m)	Hydraulic Conductivity (m/s)
1	8.7	2.90E-09
2	15.3	3.80E-10
3	19.7	1.20E-10
4	24.8	1.30E-10
5	32	5.00E-11
6	43.7	5.45E-11
7	52.5	8.20E-11
8	69.7	2.20E-11
9	79.7	1.30E-07
10	85.17	1.00E-06
11	94	1.00E-07
12	100.1	1.30E-06
13	108.8	1.30E-07
14	118.8	1.10E-09
16	141	1.40E-10
17	147.4	6.90E-11
18	157	4.90E-09

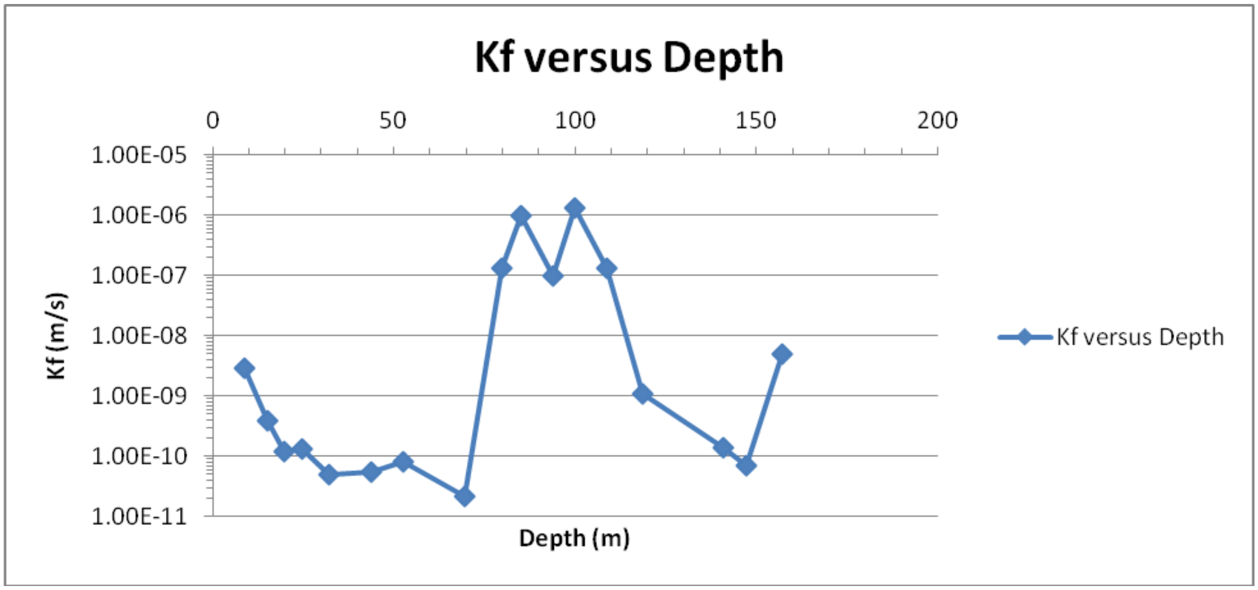

Figure 16: Graph for hydraulic conductivity (Kf) versus depth.

4.3.2 Hydraulic conductivity estimated from sediment texture

In addition the grain size distribution of the same 18 samples has been used to calculate hydraulic conductivity using the Seelheim (1880) method (figure 15). The grain size distribution has been determined with a conventional dry sieving technique. The results are shown in table 4. This method has been used to compare the actually measured hydraulic conductivities by the falling methods with those estimated by the sediment texture. The calculated hydraulic conductivity shows a discrepancy to the Kf values obtined by the falling head permeameter tests. This discrepancy is discussed in chapter 5.Cumulative frequency versus grain diameter curves were obtained for every sample (appendix 2).

Table 3: Hydraulic conductivity calculated from the grain size distribution using the Seelheim method (1880).

Sample no.	Sample depth (m)	Hydraulic Conductivitiy (m/s)
1	8.7	1.20E-04
2	15.3	3.20E-04
3	19.7	1.20E-04
4	24.8	1.30E-04
5	32	1.40E-04
6	43.7	1.10E-04
7	52.5	1.10E-04
8	69.7	1.10E-04
9	79.7	1.10E-04
10	85.17	1.10E-04
11	94	1.10E-04
12	100.1	1.10E-04
13	108.8	1.10E-04
14	118.8	1.10E-04
16	141	1.00E-04
17	147.4	1.00E-04
18	157	6.00E-05

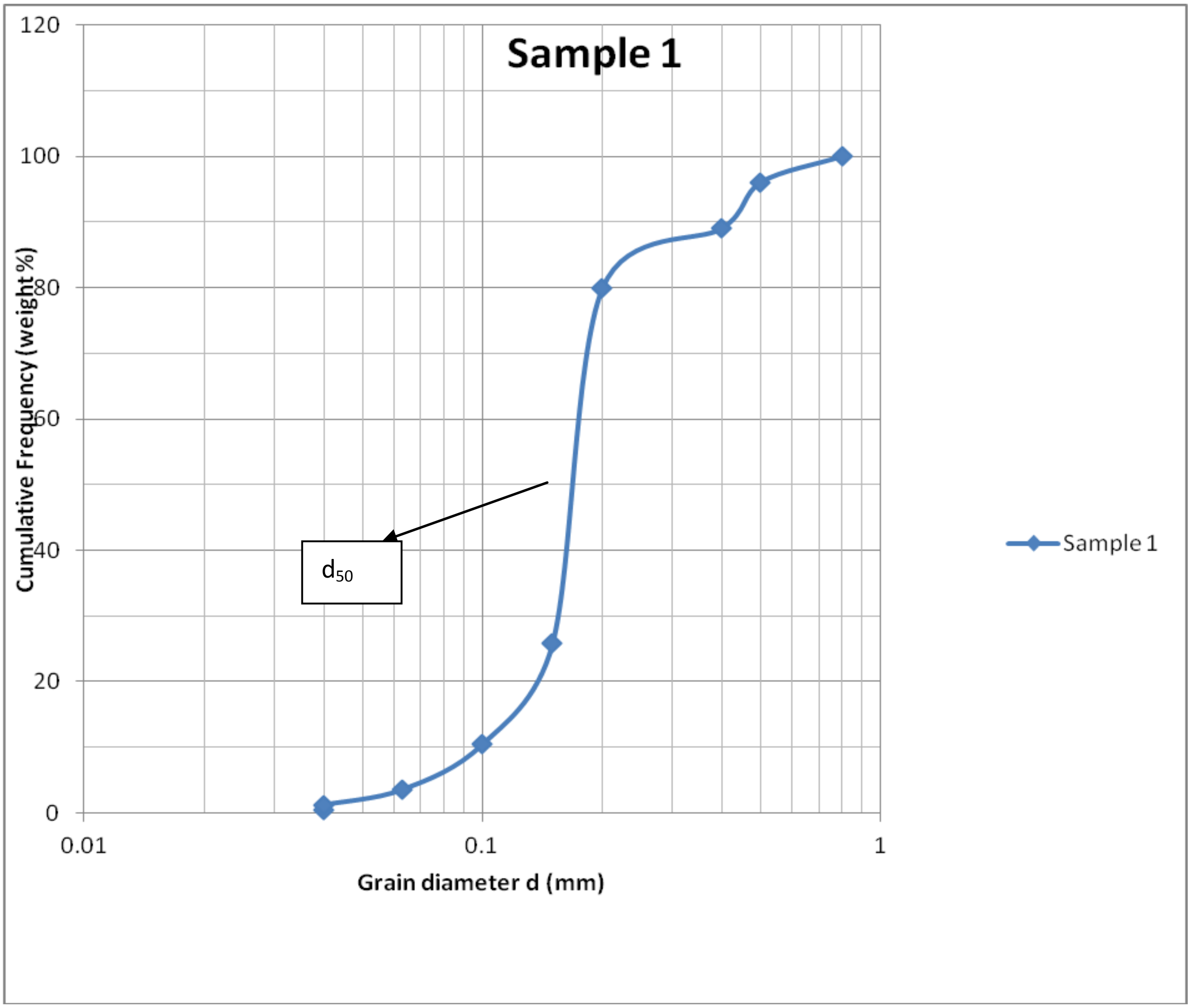

Figure 17: kf value obtained from sieving analysis.

CHAPTER 5: DISCUSSION

5.1 Introduction

This chapter consists of the interpretation of results presented in the previous chapter. The findings of the study have been compared and linked to observations and interpretations found in related literature.

5.2 Hydraulic conductivity in relation to sediment texture

The hydraulic conductivity results delineate the aquifers/leaky aquifers and aquitards/aquicludes found in the borehole. The upper 8.7 m of the core was, however, missing due to drilling problems. It was observed that these 8.7 m of the core likely belongs to the highly permeable perched aquifer and hence high hydraulic conductivity results must be expected. Downward, the perched aquifer is followed by an aquiclude layer, which according to BIWAC (2006) is located between the perched aquifer and the Ohangwena 1 (KOH 1) aquifer. The falling head method was used to produce hydraulic conductivity results from 8.7 m depth to 159 m depth. The results show that the aquiclude layer starts at 8.7 m with a hydraulic conductivity of 2.90E-09 m/s to a depth of 69.7 m where the hydraulic conductivity is 2.20E-11 m/s. Within this interval the hydraulic conductivity varies between 3.80E-10 m/s and 8.20E-11 m/s, showing that the material is largely impermeable and hence classifies as an aquiclude.

According to the hydraulic conductivity results obtained, the Ohangwena 1 (KOH-1) aquifer starts from a depth of 69.7 m with a hydraulic conductivity of 1.30E-07 m/s to the depth of 141.1 m where the hydraulic conductivity is 1.40E-10 m/s. From there the hydraulic conductivity starts dropping again downwards (figure 14) indicating a deeper aquiclude. This interval is likely the aquiclude between KOH-1 and KOH-2.

An important point to mention is that the hydraulic conductivities measured in KOH-1 are too low to classify KOH-1 as a typical aquifer. According do DIN 4049-5 standard classification the kf range from 1.0 E-05 m/s to 1.0 E-08 m/s applies to aquitards and leaky aquifers. As all kf values measured in KOH-1 fall in this interval, KOH-1 should rather be termed a leaky aquifer.

A sieving analysis was carried out to estimate theoretic hydraulic conductivities based on sediment texture, and to compare those with the hydraulic conductivities obtained from the falling head method. The hydraulic conductivity results obtained from the falling head method are considered to yield more realistic results for this project as explained below: The theoretic texture related conductivties were calculated by applying the Seelheim method (1880) to cumulative frequency curves of grain-size distributions. The results range from 3.20E-04 m/s to 6.00E-05 m/s of the entire 159 m depth of the core (Table 4). These results are representing significantly higher hydraulic conductivities compared to those obtained from the falling head method, indicating more permeable intervals. This discrepancy can be explained by the sample preparation for the sieving: The samples were partly semi-consolidated due to the presence of calcrete and dolocrete, and therefore they had to be mechanically crushed prior to sieving, and herewith the texture of the test material had been significantly altered from its original state. Another factor to explain higher permeabilities calculated from grain-size distributions is the likely presence of complex-layer clay minerals such as smectite clays that swells when saturated with water and shrink when dried out. Samples had to be dried prior to sieving, leading to the shrinkage of the smectite clays. Therefore the clays appeared underrepresented in the sieving analysis and herewith calculated hydraulic conductivities are higher.

According to Walzer's (2010) litholog of borehole WW201047 KOH-1 comprises greenish, semi-consolidated sandstone, while KOH-2 comprises mainly red sandstone and clay. The observed lithology of borehole WW203302 is slightly different with KOH-1 of Walzer (2010) as it includes very light yellow sand, fine-medium grained with minor silt, with white hard calcrete/ dolocrete nodules and different phases and degrees of bioturbation.

Boreholes located some 80 to 100 km farther south of WW203302 also intersect the Ohangwena aquifers. Ananias et al. (2012) analyzed pumping test data to calculate hydraulic conductivity for KOH-1 using the Theis method. The hydraulic conductivities range from 1.60E-4 m/s to 8.0E-6 m/s. These results show slightly higher conductivities compared to those obtained for KOH-1 at the study borehole WW203302 obtained using the falling head method (ranging from 1.0E-6 m/s to 1.3E-7 m/s). Though very similar, these differences in the hydraulic conductivities obtained from pump tests of the southern boreholes compared to the results obtained from the falling head of the study borehole can be explained by the different methods used to obtain the hydraulic conductivities. In addition lateral inhomogeneity of KOH-1 may contribute to the variation in hydraulic conductivity.

5.3 Porosity estimation based on sediment texture

The laboratory porosity results for the samples were not made available during the period of this project; therefore the porosity has been estimated by using literature values for similar sediments. The core is made up medium to very-fine grained unconsolidated sand that is moderately to poorly sorted. The typical effective porosity of such sands with no cement would be approximately 30% to 35%, however, the study core material contains calcrete and dolocrete cementation and minor silt and clay, therefore, the porosity values must have benne significantly reduced and hence a porosity value of 20% was used.

5.3 Groundwater recharge of KOH-1

One important research question was, whether or not there is leakage from the perched aquifer KOH-0 to KOH-1. Various calculations were carried out to assist answering this question and develops possible ideas of where else could be recharge to the KOH-1 aquifer. The following calculations were carried out:

Calculation of vertical groundwater movement from the shallow perched aquifer through the aquitard down to the confined aquifer KOH-1 was calculated using the procedure shown in figure 18. Hydraulic conductivity over the entire aquiclude thickness was calculated, as it one of the required parameters needed to calculate the distance velocity.

Distance velocity was calculated using the formula:

Va= [(Kf*dh/L)/ne]

Where:

Va (m/s) = distance velocity

Kf (m/s) = hydraulic conductivity

dh (m) = change in hydraulic head

L (m) = length of aquiclude (top of KOH-1 – base of KOH-0)

Ne = effective porosity (fraction of 1)

The Hydraulic conductivity over the entire aquiclude thickness was calculated using the formula:

Kf = (Kf-1*L-1+ Kf-2*L-2+ Kf-3*L-2+Kf-n*L-n)/ (L-1+ L-2+ Ln)

Inserting the measured values in the equation gives:

Kf=[(2.9E-9 m/s*6.6 m) + (3.8E-10 m/s * 4.4 m) + (1.2E-10 m/s* 5.1 m)+ (1.3E-10 m/s*7.2 m) + (5E-11 m/s * 11.7 m) + (5.45E-11 m/s *8.8 m) + (8.2E-11 m/s* 17.2 m) + (2.2E-11 m/s*10 m)] / [6.6 m + 4.4 m + 5.1 m + 7.2 m + 11.7 m + 8.8 m + 17.2 m + 10 m]

=3.5E-10 m/s

Distance velocity (Va) = [(3.5E-10 m/s)* (60 m- 4 m)]/0.2

= 1.77E-9 m/s = **5.5E-2 m/year**

Knowing the velocity at which the water travels through the aquiclude and the distance travelled at this velocity, we can calculate for the time the water takes to travel through the aquiclude with a distance (thickness) of 61 m at the velocity calculated by using the following formula:

Time = Distance travelled by the water/ velocity at which the water is flowing

Therefore;

Time = (61m) / (1.77E-9 m/s)

= 34560906515.6 seconds = **1096 years**

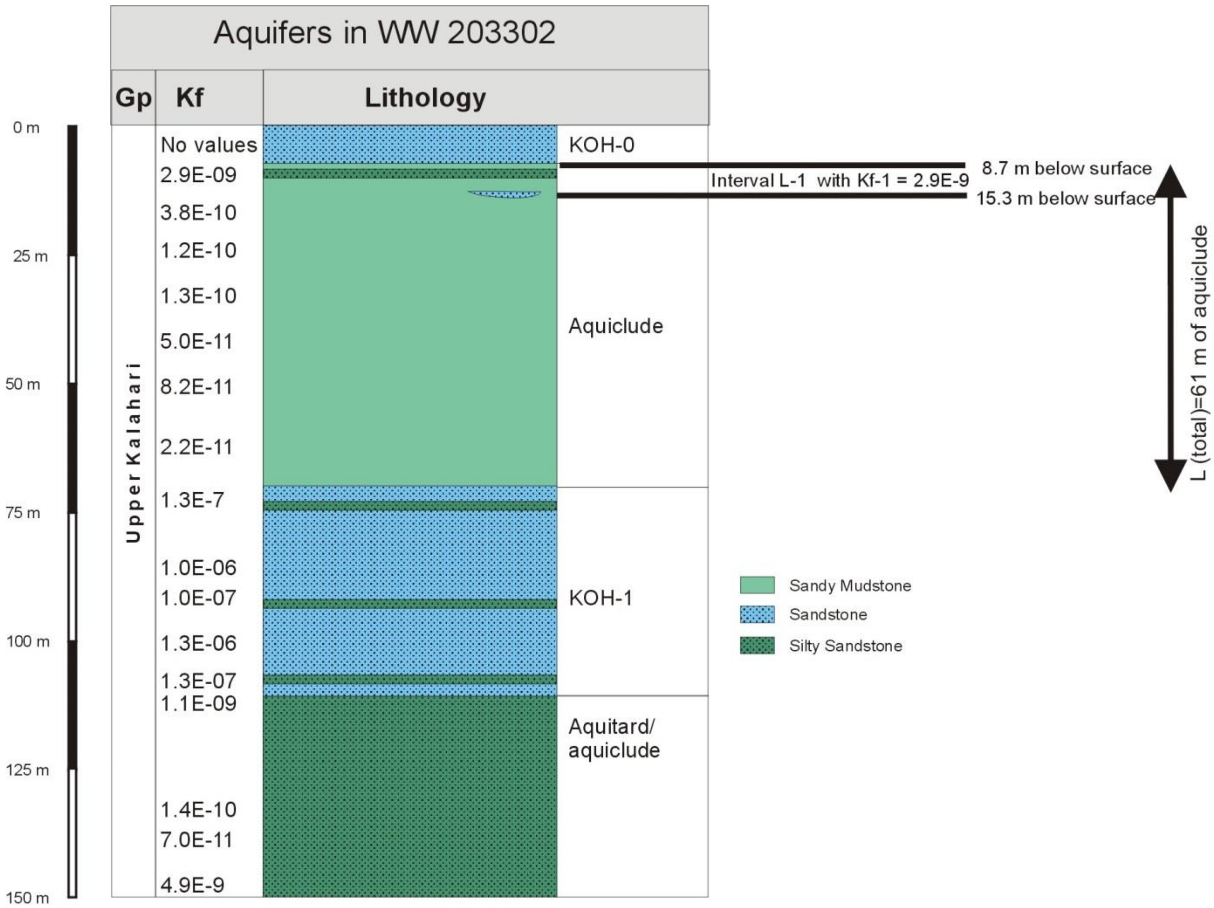

Kf (m/s): Hydraulic conductivity
h (m): hydraulic head
L (m): top KOH-1 - base KOH-0
ne: effective porosity (fraction of 1)
Va (m/s): distance velocity

Kf over entire aquiclude thickness:

Kf = (Kf-1*L-1 + Kf-2*L-2 + Kf-n*L-n +...) / (L-1 + L-2 + Ln)

dh = h2-h1

h1= 5 m
h2 = 67 m
(values obtained from nearest neigbouring borehole)

Va (m/s): {kf *(dh/L)}/ne

Figure 18: Schematic log of Aquifers and Aquitard

According to Walzer (2009) the water in KOH-1 becomes brackish to saline towards the south with a distance of a few kilometers and it is therefore not developed for human consumption. The southwards directed salinity increase may be partly explained by input of more saline water deriving from the southern perched aquifer which tends to be significantly more saline than the norther perched aquifer. So far there is limited leakage from the perched aquifer to KOH-1 according to the velocity and travel time calculation made above. Though, the leakage takes over a thousand years at a very low velocity to reach KOH-1, this can be sufficient enough to have contributed to the salinity of KOH-1. Figure 19 provides a simplistic model for explaining salinity increase in the southern KOH-1 by saline water input from KOH-0. It should be emphasized that the situation is like much more complex as ephemeral flooding of saline pans, and the possible presence of fossil groundwater that accumulated during different climates need to be considered.

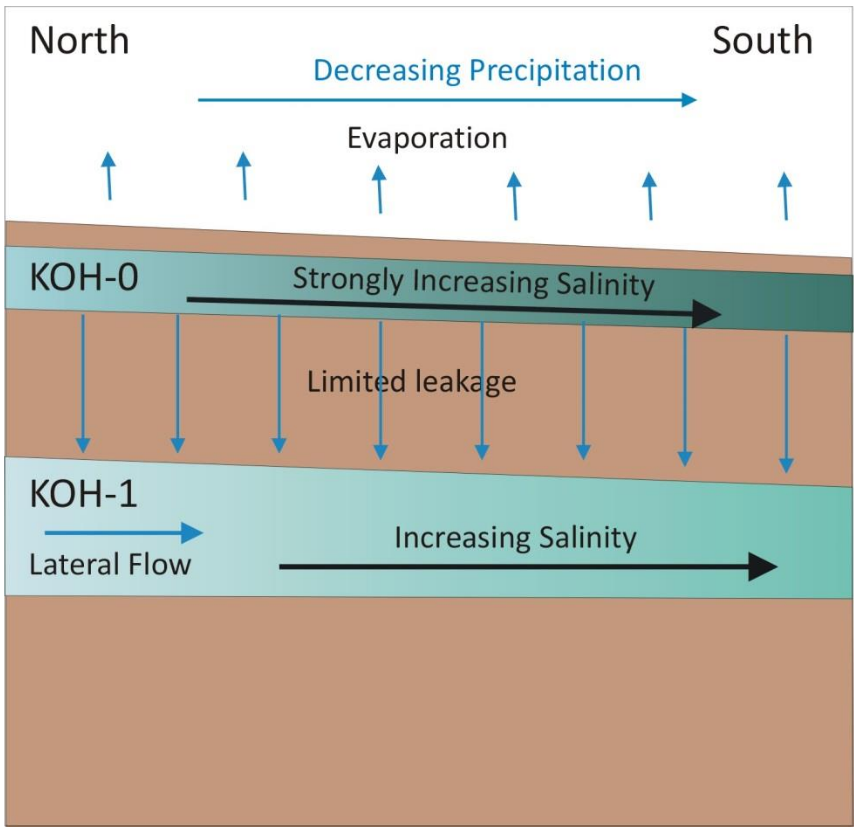

Figure 19: Simplistic model to explain saline water input from the southern sections of KOH-0 into KOH-1.

CHAPTER 6: CONCLUSIONS AND RECOMMENDATIONS

The main objectives of this study is to produce a core documentation/core log on principal lithological characteristics from 0-150 m depth of the core and to establish the hydraulic parameters (porosity and hydraulic head/permeability) of aquifers/leaky aquifers and aquicludes/aquitards in the samples taken.

The hydraulic conductivity results, obtained using the falling head method, delineate the depth intervals of aquitards, aquicludes and the leaky aquifer KOH-1. An aquiclude exists at the depth from 8.7 m to 69.7 m with very low hydraulic conductivity. At the depth interval fron 79.9 m to 108.8 m hydraulic conductivities are higher. This interval delineates KOH-1; kf values classify the latter as a leaky aquifer.

KOH-1 is likely to receive some recharge by vertical inflow deriving from the leaking perched aquifer KOH-0. This recharge is limited due to the low distance flow velocity of 1.7675E-9 m/s, and it takes over 1000 years for water from the perched aquifer to pass through a 61 meters thick of low conductive aquiclude to reach KOH-1.

Considering the hydrogeological setting probably most of the water for KOH-1 derives from farther (north), the southern Angolan catchment.

Recommendations

This study is based on one borehole only, therefore the data on which the conclusions are based are rather limited and the conclusions may be biased and misleading. Therefore a regional study that includes more hydraulic data from adjacent boreholes is recommended. In addition a regional map of hydraulic heads for KOH-1 would enable to produce a consistent groundwater flow model. The latter will finally conclude on the possible recharge from a proposed groundwater catchment farther north in Angola.

BIBLIOGRAPHY

- Akanegbu, J.O., 2013.Comparizon of Different Methods of Measuring Hydraulic Conductivity in Drained Peat Soils using Drainmod as a Verification Tool. MSc Thesis, Department of Process and Environmental Engineering and Water Resources, University of Oulu. pp 116.

- Ananias, A.L., 2012. An estimation of the transmissivity values of the Ohangwena I and II Aquifers in the Ohangwena region, BSc Honours Thesis, Geology Department, University of Namibia, pp 84.

- Bittner, A.F.W., Kleczka, M.L., 2006. Desk Study Report: Cuvelai-Etosha Groundwater Investigation, Bittner Water Consult, Windhoek, Namibia.

- Lindenmaier,F., Miller,R., Fenner,J., Christelis,G., Dill,H.G., Himmelsbach ,T., Kaufhold,S., Lohe,C., Quinger., Schildknecht,F., Symons,G., Walzer,A., Van Wyk,B. 2014. Structure and genesis of the Cubango Megafan in northern Namibia: implications for its hydrogeology: Hydrogeology Journal, v 22, pp 1307-1328.

- Mendelsohn, J., El Obeid, S., Roberts, G., 2000. A profile of north-central Namibia. Environmental profiles project. Gamsberg Macmillan Publishers, Windhoek, 80 pp.

- Miller, R., 1983. The Pan-African Damara Orogen of South West Africa/Namibia. Johannesburg: Special publication / Geological Society of South Africa. Pages 431–515.

- Miller, R., 1997. The Owambo Basin of Northern Namibia. Chap. 11, pages 237– 268 of: Sellly, R.C. (ed), African Basins. Sedimentary Basins of the World. Amsterdam: Elsevier Science B.V.

- Miller, R, 2008c. The Geology of Namibia. Vol. 3. Windhoek: Geological Survey Namibia. Ministry of Mines and Energy.

- Miller, R., 2009 (June). Expert in Namibian geology, Geological Survey of Namibia.

- Momper, J., 1982. The Etosha Basin re-examined. Oil & Gas Journal, 5, 262–287.

- Schaller, T., 2012.Hydrogeochemical Study of the Multi-layered Ohangwena Aquifer in North Central Namibia. MSc Thesis, Faculty of Physics and Geoscinces, University of Leipzig.

- Walzer, A., 2009. Multilayered Aquifers in the Central-North of Namibia and their Potential Use for Water Supply, Technische Universität Dresden, Bundesanstalt für Geowissenschaften und Rohstoffe .

Appendices

Appendix 1 : Description of geological log of WW203302 (Logging done by miller 2015)

Depth to m	Core recovery m	Core loss m	Core description	Bioturbation
0-8.5	No core collected			
-9	0.5	0	Very light yellow sand, fine grained with rare coarse grained sand, unbedded, poor to variable sorting. Most medium to coarse sand are very well rounded from 9m downwards, consists of soft calcrete cement and hard.	
-10	1	0	Very light yellow sand, fine to medium sand, minor silt, poorly sorted, hard with dolocrete cement. More uniform reddish hematite cooler with minor layers of clayey sand and very thin white cross-cutting veinlets of dolocrete.	
-11	1	0	Very light yellow sand, fine to medium grains, minor silt, poor sorting, hard with dolocrete cement.Have a more uniform reddish hematite colour,very thin white cross-cutting veinlets of dolocrete and softer layers of clayey sand.	
-11.5	0.5	0	Very light yellow fine to medium sand with minor silt, rare coarse grains, poor sorting, hard with dolocrete cement. Uniform reddish hematite cooler	Faint bioturbation
-12.5	1	0	Very light yellow fine to medium sand with minor silt, scattered coarse grains, poor sorting, softer then above layer, calcrete cemenented.Uniform reddish hematite cooler. Tiny filigree networks of Mn staining	Variously calcrete cement bioturbation

Depth to m	Core recovery m	Core loss m	Core description	Bioturbation
-13.5	1	0	Very light yellow fine to medium sand with minor silt, rare coarse grains, poor sorting, hard with dolocrete cement. Uniform reddish hematite cooler	Root bioturbidation at 12.82 m and fint bioturbidation channels in the last 20 cm.
-14.5	1	0	Very light yellow sand, fine to medium grained with minor silt, scattered coarse grains, rare granules, very poorly sorted and semi-consolidated. Calcrete cemented, ferruginised, remnant patches of the original cooler and bleached post-ferruginisation veins at various meters.	Red bioturbidation at 13.59-13.67 m, zoned rhyzolith at 13.80 m with white margin of dolocrete cement.
-15.5	1	0	Very light yellow sand, fine to medium grained with minor silt. Scattered coarse grains, rare granules, very poorly sorted, semi-consolidated with dolocrete cement, horizontal 1mm thick white clay layer at 15.17 m and a 2 cm thick horizontal calcrete vein at 14.85 m,ferruginisation becoming patchy	Scattered bioturbidation throughout, small round bioturbidation patches near base ,good rhyzolith at 15.04 m
-16.5	1	0	Very light yellow sand, medium to fine grained, semi-consolidated with weak dolocrete cement.Ferruginisation decreasing downwards, horizontal calcrete veins at 15.9 m with thin bleached carbonate free margins	Red bioturbibation ,good red bioturbation channels at 15.6 and 16.04 m
-17.5	1	0	Very light yellow sand, becoming finer grained downwards,semi-consolidated,weak dolocrete cement becoming softer and less consolidated downwards, white calcrete nods at 16.68 m	Minor ferruginisation bioturbidation decreasing downwards

Depth to m	Core recovery m	Core loss m	Core description	Bioturbation
-18.5	1	0	Very light yellow sand, fine to medium grained with minor silt, scattered coarse grains, rare granules, semi-consolidated with dolocrete cement	
-19.5	1	0	Fine to medium grained sand with minor silt and very rare coarse grains.	
-20.5			Very light yellow sand, fine to medium grained with scattered coarse grains and granules up to 0.8 cm diameter from 19.5-20.05 m becoming fewer and smaller downwards. poor sorting of medium sand,semi-consolidated,dolocrete cemented. Consists of a few tiny soft white calcrete nods	Faint bioturbidation in places
21.5	1	0	Very light yellow sand, fine to medium gains with minor silt, very rare coarse grains, air sorting ,semi-consolidated by dolocrete cement, small fragments of medium grey-brown clay from 20.5-20.9 m,vertical 10 cm thick long calcrete nodule at 21.10 m.	Small fragments of medium grey-brown clay, probably from a thin clay layer fragmented by the bioturbidation, faint bioturbidation below this
22.5	1	0	Very light yellow sand, fine to medium grained with minor silt, slightly finer than above metre, very rare coarse grains, fair sorting, semi-consolidated by dolocrete cement. White calcrete nodules below this.	Faint bioturbidation throughout
23.5	1	0	Same as above, fair sorting, semi-consolidated , cm white calcrete nodules at 23.08	

Depth to m	Core recovery m	Core loss m	Core description	Bioturbation
24.5	1	0	Very light yellow sand, fine to medium grained with minor silt, a few scattered coarse and very coarse grains from 23.523.8 m.Fair sorting and semi-consolidated.	Slightly darker yellow bioturbidation from 23.63-24.25 m
25.5	1	0	Very light yellow sand, fine to medium grained with very minor silt, rare coarse grains, fair sorting, semi-consolidated	Faint but scattered bioturbidation
26.5	1	0	Very light yellow sand, fine to medium sand, minor silt, sorting poorer, semi-consolidated	Some faint bioturbidation to 26.96 m
27.5	1	0	Very light yellow sand, medium to fine grained, minor silt and very scattered coarse grains. Fair sorting, semi-consolidated but soft. Small hard white calcrete nodules.	Some faint bioturbidation to 27.86 m
28.5	1	0	Similar to previous metre but more silty, poorer sorting, soft and has a few tiny soft white calcrete spots.	Faint bioturbidation scattered throughout
29.5	1	0	Very light yellow sand, medium to fine grained, very minor silt .rare scattered coarse grains, air sorting, has a 2 cm thick layer of many tiny white calcrete nodules at 29.12 m,rare 1-2 cm ferruginous spots	Faint bioturbidation from 27.5- 28.17 m, ferruginous spots may be bioturbidation
-31.5	1	0	Same as for 28.5-29.5 m layers; with some hard white calcrete nodules and very small soft calcrete nodules	Open vertical cavity with very fine grained and slightly ferrugious wall lining from 30.8-30.88 m

Depth to m	Core recovery m	Core loss m	Core description	Bioturbation
-32.5	1	0	Same as for 28.5-29.5 m layers; long hard irregular white calcrete nodule from 31.58-31.70 m	Very faint, slightly ferruginous vertical bioturbidation channels at 31.62, 31.94-32.22, and 32.45 m
-33.5	1	0	Vey light yellow sand, medium to fine grained with minor silt but more than above layers. Very rare coarse grains, air to poor sorting, semi-consolidated and contains a few small hard and soft whit calcrete nodules.	Faint bioturbidation at 33.32 m
-34.5	1	0	Very light yellow sand with very minor silt, fair sorting,semi-consolidated,scattered tiny soft white calcrete nodules, aggregate of small hard calcrete nodules at 34.36	Long, thin bioturbidation tube filled with white calcrete from 33.53-33.6, faint slightly ferruginous bioturbidation at 34.06, 34.18 m, scattered faint bioturbidation
-35.5	1	0	Very light yellow sand, fine to medium grained, very minor silt and poor sorting	
-36.5	1	0	Very light yellow sand, medium sand with trace silt, very rare coarse grains, fair sorting, semi-consolidated but soft.	vertical bioturbidation burrow from 35.7-35.84 m, minor faint bioturbidation in places
-37.5	1	0	Same as above layer but slightly more silt	

Depth to m	Core recovery m	Core loss m	Core description	Bioturbation
-38.5	1	0	Same as above but variable concentrations of main fraction from medium sand to fine sand.	Hollow root tube at 37.02 m; faint bioturbidation from 37.9-38.06 m
-39.5	1	0	Very light yellow sand ,fine to medium grained with very minor silt ,its soft with a large white hard calcrete nodule at 39.30 m	3 phases of bioturbidation, 1st phase is very faint, 2nd phase is long vertical with slight ferruginous burrow from 38.7-38.91 m, 3rd phase has red ferruginous burrow from 38.74-38.91m
-40.5	1	0	Same as above layer but it is mainly fine sand and most grains are still very well rounded	Some scattered faint bioturbidation channels
-41.5	1	0	Same as above layer but has four small isolated white calcrete nodules	Thin hollow tube-like cavity at 40.96 m, faint bioturbidation at 41.2 m
-42.5	1	0	Same as above layer but contain trace silt and Calcrete nodules	Faint bioturbidation at 42.22 m, thin calcrete streak at 42.30 m

Depth to m	Core recovery m	Core loss m	Core description	Bioturbation
-43.5	1	0	Same as above layer but contains, rare scattered coarse grains	Two long thin calcrete nodules at 42.62-42.76 m & 42.93-43.02 m (latter nodular) – possibly filling of bioturbidation channels or rhyzoliths; one red bioturbidation burrow at 43 m; 1 0.8 cm Ø wood of root with bulk edge at 43 m
-44.5	1	0	Same as above layer but its mainly medium sand with clayey sand spots and streaks	Long thin irregular, knobbly calcrete nodules from 44.03-44.11 & 43.72-43.86 m, very light green spots may be bioturbidation, faint bioturbidation in places
-45.5	1	0	Same as above layer but mainly medium sand with some small calcrete nodules	One small reddish bioturbidation feature at 44.92 m
-46.5	1	0	Same as above but trace silt with some hard calcrete nodules	Single reddish bioturbidation features at 45.63, 45.8, 46.1 m, faint bioturbidation throughout

Depth to m	Core recovery m	Core loss m	Core description	Bioturbation
-47.5	1	0	Same as above but mainly fine sand with less medium sand ,very minor silt, fair sorting and have some calcrete nodules	Subtle colour differences in very light yellow suggest extensive bioturbidation throughout
-48.5	1	0	Same as above	Bioturbidation as above but very faint
-49.5	1	0	Same as above ,contains a large calcrete nodule at 49.13-49.2 m	Bioturbidation from 49.23-49.28 m, wood of thin root at 49.24-49.28 m
-50.5	1	0	Same as above ,with trace silt and a few hard white dolocrete nodules	Very light olive bioturbidation spots with small white calcrete
-51.5	1	0	Same as above with small calcrete and dolocrete nodules ,one zoned calcrete dolocrete nodules with calcrete margin,	Thin very light grey bioturbidation channels from 51.0-51.45 m,faint bioturbidation throughout, 1 calcrete-cored spot as above
-52.5	1	0	Same as above with very minor to trace silt with nods as above	Bioturbidation as above from 51.5-51.75 m, some Y-shaped channels; strange little bioturbidation channels at 52.2 m
-53.5	1	0	Fine sand ,silt with very minor medium sand ,fair sorting ,large hard calcrete nodule at 52.99 m,1 small hard calcrete nodule	A few thin very light grey channels in places through whole core, some Y shaped

Depth to m	Core recovery m	Core loss m	Core description	Bioturbation
-54.5	1	0	Same as above with trace silt ,fair sorting	Very faint y bioturbidation t, some very light grey bioturbidation throughout
-55.5	1	0	Same as above with minor medium sand and trace silt with some calcrete nodules	Faint bioturbidation in several places
-56.5	1	0	Same as above	Very faint yellow bioturbidation throughout
-57.5	0.96	1st 6 cm	Same as above with some small hard Calcrete nodules, one flat clast of dark brown grey clay at 57.72 m	Some very faint yellow bioturbidation
-58.5	1	0	Same as above, zone of many small white dolocrete nodules from 57.88-58.06 m, 2 hard white calcrete nodules	Faint bioturbidation in zone of small nodules, some channels calcified, ditto at 58.4 m
-59.5	1	0	Same as above	Very faint yellow sand-filled bioturbidation channels at 59.4 m, thin very light grey bioturbidation channels filled with clay-rich sand from 58.9-59.0 m; faint bioturbidation throughout
-60.5	1	0	Same as above with a few scattered coarse grains, soft	Some very light yellow bioturbidation
-61.5	1	0	Same as above with some hard calcrete nodules	Some very light yellow bioturbidation

Depth to m	Core recovery m	Core loss m	Core description	Bioturbation
-62.5	1	0	Same as above with some hard calcrete nodules	Some very light yellow bioturbidation
-63.5	1	0	Fine to minor medium sand, minor to very minor silt, consolidated with some porosity reducing calcrete cement from 62.5-62.9 m ,large hard calcrete dolocrete nodule from 62.9-62.96 m.Below this the layer have softer fine sand with minor medium sand ,trace silt and fair sorting	
-64.5	1	0	Fine to medium sand ,trace silt ,fair sorting ,hard with dolocrete/salt cement ,many calcrete dolocrete nodules up to 4 cm in diameter,particulary from 63.9-64.1 m.	
-65.5	1	0	Same as above but silt fewer and up to 2 cm in diameter	
-66.5	1	0	Same as above, hard ,consolidated, dolocrete cement with some calcrete dolocrete nodules	Some faint yellow bioturbidation
-67.5	1	0	Same as above with a few hard calcrete dolocrete nodules to 67 m, hard calcrete nodules below this	Abundant very light yellow bioturbidation, very clear from 67.0-67.4 m
-68.5	1	0	Same as above with several calcrete dolocrete nodules	Faint very light yellow bioturbidation from 67.5 m, best from 68-68.25 m, none below this

Depth to m	Core recovery m	Core loss m	Core description	Bioturbation
-69.5	0.98	68.50-68.52	Same as above with several calcrete dolocrete nodules, very light yellow ,soft faint bedding from 69.63-69.71 m	Very faint bioturbidation
-70.5	1	0	Same as above slightly softer but still well consolidated ,with several calcrete dolocrete nodules	Very faint bioturbidation throughout, best from 70.0-70.2 m
-71.5	1	0	Same as above with irregularly shaped calcrete dolocrete nodules from 71.3-71.42 m	Very light yellow bioturbidation throughout, U-shaped channel lying on side at 71.1 m
-72.5	1	0	Same as above ,much softer, some washed out from drilling	Very faint light yellow bioturbidation
-73.5	1	0	Same as above with softer and harder zones, some wash out from drilling, some calc dc nods, core very disturbed	
-74.5	1	0	Same as above much wash out from drilling, core very disturbed	
-75.5	1	0	Same as above, patchy harder and softer parts, partial drilling wash out of softer parts, 1 calcrete dolocrete nodules, core very disturbed	
-76.5	1	0	Fine to very fine sand with very minor to trace silt, softer and sticky. Core very wet from 71-76 m	
-77.5	1	0	Same as above,soft.calcrete dolocrete nodules at 76.7 and 77.35 m,large dolocrete, large dolocrete nodules at 76.85 and 77.0 m	Faint bioturbidation at 77.3 m

Depth to m	Core recovery m	Core loss m	Core description	Bioturbation
-78.5	1	0	Fine to medium sand ,trace silt, fair to well sorted ,soft ,1 small calcrete dolocrete nodules, core disturbed in places	Bioturbidation from 77.6-77.7 m
-79.5	1	0	Same as above, more consolidated, proportion fluvial grains (shiny and not like Aeolian grains) increasing	Very faint very light yellow bioturbidation, 1 slight ferruginous channel at 79.2 m
-79.8	0	0.3	Core loss	
-81.7	1	0.9	Fine to medium sand, with trace silt, air to good sorting ,soft with 2 small calcrete dolocrete nodules core disturbed in places	
-82.6	1	0.1 m gain	Same as above, most grains shiny (fluvial), soft, very light yellow, 4 small calcrete dolocrete nodules	Very faint slight ferruginous bioturbidation at 82 m, Red bioturbidation spots at 87 cm
-84.6	1	1	Same as above ,soft,2 large calcrete dolocrete nodules, one at 84.6 m,core a bit disturbed	Faint bioturbidation, rare small bioturbidation spots
-85.75	1	0.15	Same as above ,1 coarse grain, sorting fair to good, soft	Faint slight ferruginous bioturbidation from 84.72-84 87 m
-87.2	1	0.45	Same as above, fair to good sorting and soft	2 bioturbidation channels in top 20 cm
-88.2	1	0	Same as above fair to good sorting and soft	Very light brown bioturbidation channels from 87.8-88.2 m

Depth to m	Core recovery m	Core loss m	Core description	Bioturbation
-90.5	1	1.3	Same as above ,fair to good sorting, still very light yellow ,soft sand, hard layer from 88.22-88.47 of dark red silcrete and light pink dolocrete nodules all totally cemented by a very light green dolocrete cement	Rare scattered bioturbidation below silcrete
-91.5	1	0	Same as above, air to good sorting ,still very light yellow ,soft upper ½ of core disturbed	
-93.3	1	0.8	Same as above most grains shiny, fair-good sorting, still very light yellow, soft, core v disturbed below 1st 20 cm	Tiny red bioturbidation spots in 1st 20 cm
-94.3	1	0	Same as above fair-good sorting, still very light yellow, soft, core very disturbed in 1st 40 cm	
-96.8	1	1.5	Same as above fair-good sorting, still very light yellow, soft, core very disturbed	
-99.3	1	1.5	Same as above ,fair to good sorting still very light yellow, soft for upper 68 cm; then 12 cm of same sand hard and cemented by dolocrete & enclosing large brown, very fine grained calcrete dolocrete nodules basal 18 cm same sand as above but mainly fine sand more silt, most grains shiny; very light yellow, soft	
-100.3	1	0	Fine to very fine sand ,more silt than above ,fair to poor sorting very very light grey yellow,soft,12 cm thick zone of calcrete dolocrete nodules at 100 m	Possible very faint bioturbidation from 99.58—99.75 m

Depth to m	Core recovery m	Core loss m	Core description	Bioturbation
-101.3	1	0	same sand, same sorting, same colour, soft as above	Some faint bioturbidation from 100.58-101.02 m
-102.8	1	0.5	Same as above but more very fine sand and soft	Some faint bioturbidation in places
-103.8	1	0	Very fine sand to fine sand, silt about 15% very minor medium sand, poor sorting and soft	Very faint bioturbidation in places
-104.8	1	0	Same as above	Very faint bioturbidation in upper ½
-105.8	1	0	Same as above	Very faint bioturbidation in places
-108	0.54	1.66	Same as above	Rare faint bioturbidation
-109	1	0	Same as above to 108.2 m then finer below, fine-very fine sand, silt (15-20%), rare medium sand grains, poor sorting, very very light grey-yellow	
-110	1	0	Same as above with ± 20% silt to 109.14 m; calcrete cemented below that with increasing cement to 109.77 m. Last 23 cm a nodular pedogenic calcrete; 1-cm thick layer of very small calcrete nodules at 109.22 m	2 bioturbidation spots at 108.94 m

Depth to m	Core recovery m	Core loss m	Core description	Bioturbation
-111	1	0	Very variable. Sand as above with ± 20% silt to 110.32 m but weakly & variable cemented by calcrete; horizontal,1-cm thick speckled layer of dark brown clay; 110.33-110.54 m:- angular fragments of massive groundwater calcrete dolocrete enclosed in very light green sand ,all cemented by calcrete nodules 110.54-110.65 m:- nods with dark brown cores of rims of calcrete dolocrete, nodules enclosed in the same very light green cemented sand; 110.65-110.77 m:- as for 110.33-110.54 m; 110.77-111.0 m:- fine sand ,clayey, very light green, salty, soft with 1-cm thick interbedded layers of very very light brown fine sand at 110.77, 110.83, 110.91 & 111.0 m	
-112	1	0	Very light green fine sand, clayey, salty ,soft to 111.6 m; nodular pedogenic calcrete dolocrete with matrix of the soft very light green clayey fine from 111.6-112 m	Bt channels filled with very very light brown fine sand from 111-111.10 m, 2 long bioturbidation channels from 110.5-110.6 m

Depth to m	Core recovery m	Core loss m	Core description	Bioturbation
-113	1	0	Very variable. Pedogenic calcrete dolocrete with it matrix of soft very light green clayey ,fine sand continues to 112.15 m but with fewer nods. 112.15-112.49 m: - Sand, that is fine, soft, very very light brown, calcrete dolocrete nodules at 112.3, 112.44 & 112.49 m. 112.49-112.58 m: - Sand that is fine, clayey, soft, very light green. 112.58-112.7 m: - Pedogenic calcrete dolocrete with it matrix of soft very light green clayey. 112.7-113.0:-fine sand, ,clayey, soft, very light green;	112-112.15 m:- Matrix may be bioturbated; 112.7-113.0 m:- Abundant whitish bioturbidation channels, no acid reaction, highly disturbed by bioturbidation
-114	1	0	Fine sand, clayey, soft, very light green	Highly disturbed by bioturbidation; 113.8-114 m:- Abundant whitish bioturbidation channels as above
-115	1	0	Fine sand, clayey, soft, very light green; large very very light tan calcrete dolocrete nodules from 114.0-114.27 m	114.47-115 m:- Clear whitish bioturbidation channels & highly disturbed by bioturbidation as above
-116	1	0	Fine sand, clayey, soft, light green to 115.8 m then lighter green to 116.10;	Bioturbidation with whitish bioturbidation channels as above to 115.7 m

Depth to m	Core recovery m	Core loss m	Core description	Bioturbation
-117	1	0	Fine sand, clayey, soft, light green from 116.1 m; 2-3 cm thick layer of small calcrete dolocrete nodules at 116.1 m; larger calcrete dolocrete nodules from 116.52-116.62 m; calcrete dolocrete layer from 116.9-117 m – this dolocrete seems to extend up into the overlying bioturbidation channels for ±8 cm	Bt with whitish bioturbidation channels as above for most of this core; note dc of 116.9-117 m extending upwards into overlying bioturbidation channels for ±8 cm
-118	1	0	Fine sand, clayey, soft, light green; scattered calcrete dolocrete nodules from 117.76-117.9 m	Bioturbidation channels throughout as above with some dolocrete cementing of bioturbidation channels in lower 8 cm
-119	1	0	Fine sand ,clayey, soft, light green to 118.61 m; 118.61-119 m hard very very light brown calcrete dolocrete with numerous irregularly shaped very light tan channel fillings of calc dc;	Same intense bioturbidation as above in green sand to 118.61 m
-120	1	0	Same calc dc continuous from 119-119.37 m; 119.37-119.48 m:- Fine Sand, clayey, soft, very light green; 119.48- 119.88 m:- Hard white massive calcrete cement with Few sandy very light tan channel fillings weakly cemented by calcrete dolocrete; 119.88-120.0 m:-fine Sand, clayey, soft, light green; 3 thin calcrete dolocrete layers	

Depth to m	Core recovery m	Core loss m	Core description	Bioturbation
-121	1	0	Fine Sand, 120-120.42 m:, clayey, soft, light green, many horizontal laminated calcrete dolocrete layers coloured white to very very light brown; 120.42-121 m:- Fine sand , clayey, light green with (i) faint horizontal bedding from 120.42-120.69 m; (ii) layers Medium Sand to-fine Sand ,very light brown sand from 120.52-120.58 & 120.82-120.94 m; (iii) 0.5 cm thick layer of green clay at 120.93 (120.95?) m	Rare small bioturbidation channels
-122	1	0	Fine Sand, with minor silt, clay, very minor medium sand, rare coarse grains, poor sorting, soft, light green; many horizontal slightly lighter fine sand layers that may be layering to 121.31 m; then same sand but with very very light green-yellow colour and only short thin subhorizontal light green streaks with occasional darker green 1-2 cm bioturbidation patches; Last 2 cm very light yellow sand with darker green bioturbidation. The very light yellow colour may be the original colour, the light green may be due to a 1st period of very pervasive bioturbidation, & the later darker green a 2nd period of bioturbidation	A bit of bioturbidation to 121.7 m, more concentrated & obvious bioturbidation from 121.7-122 m.

Depth to m	Core recovery m	Core loss m	Core description	Bioturbation
-123	1	0	Sand same as above clay, very minor medium sand, rare coarse grains, poor sorting, soft, very light yellow with 2nd period darker green bioturbidation to 122.06 m, then light green to abundant darker green bioturbidation to 122.57 m then very light yellow with abundant darker green bioturbidation to 122.64 m, light green to with abundant darker green bioturbidation to 122.80 m, then large calcrete dolocrete nodules 122.8-122.86, then same sand with uniform light green colour to 123 m; calcrete dolocrete nod at 122.4 & a few small nods from 122.61-122.70 m	light green bioturbidation may be due to a 1st period of very pervasive bioturbidation, & the later darker green a 2nd period of bioturbidation, latter abundant to 122.86 m, none below this
-124	1	0	As above to 123.10, then medium sand, minor silt, clayey, poor sorting, soft; uniform light green with very subtle colour variations suggestive of v pervasive 1st period bioturbidation to 123.73 m, then a more yellow colour to the sand with the light green bioturbidation more patchy & more obvious as bioturbidation to 124 m; darker green 2nd period bioturbidation rare; a long thin white bioturbidation channel at 123.97 m	

Depth to m	Core recovery m	Core loss m	Core description	Bioturbation
-125-	1	0	Medium to silt sand clayey, poor sorting, lt's green to 124.67 m, then green colour starts fading downwards & colour gradually becomes very very light brown to 125 m, soft; scattered small hard irregularly shaped dolocrete nodules. Light green very uniform – 1st period bioturbidation?a few scattered 2nd period darker green channels in this. Cluster of darker green channels from 124.67-124.7 m where sand colour starts to change, below this darker green channels scattered, none below 124.93 m in very very light brown sand	
-126	0.62	0.38	125-125.22 m:- Fine to medium sand, minor silt, clay, trace coarse grains, poor sorting, soft, rare 2nd period darker green bioturbidation channels 125.22-125.27 m:- Sand as above, very very light green to very very light brown, abundant 2nd period darker green bioturbidation channels; 125.37-125.62 m:- Sand as above, same very very light brown sand, hard and dolocrete cemented, so intensely pervaded by 2nd period darker green bioturbidation channels than patches of sand of original colour are rare; some bioturbidation channels filled with white calcrete cemented sand; large irregularly calcrete dolocrete nodules at each end of this section	

Depth to m	Core recovery m	Core loss m	Core description	Bioturbation
-127	1	0	Clay, slightly silty, green, hard, more sandy from 126.80-127 m; zone of irregularly dolocrete nodules from 126.92-127 m; small irregularly dolocrete nodules and patches & a few thin short horizontal and vertical dolocrete streak throughout the clay	2 long bioturbidation channels intersecting at 90° at 126.86 m
-128	1	0	Sand, very clayey, medium sand, silt, sorting poor, green; clusters of dolocrete nodules from 127.20-127.33, 127.36-127.65, 127.9-128 m; soft where no nodules	
-129	1	0	Fine Sand, minor silt, very clayey, green; abundant small round calc dc nods from 128-128.34 m which may be filled by bioturbidation channels, fewer and more irregular nodules to 128.78 m, then cluster of irregular nodules to 129 m, hard	
-130	1	0	Fine to very fine sand with minor silt, very clayey, very minor medium sand, poor sorting, green, soft; abundant small to medium irregular shaped calcrete dolocrete nodules	
-131	1	0	Sand as above to 130.15 m but fewer nodules & with some darker green bioturbidation channels; sand more clayey to 131 m, green – light green, soft, with very abundant small, mainly round calcrete dolocrete nodules	Some darker green bioturbidation channels to 130.15 m

Depth to m	Core recovery m	Core loss m	Core description	Bioturbation
-132	1	0	Sand as above, Fine to very fine sand, minor silt, very clayey with very minor medium sand. Light green, soft with abundant small to medium irregular shaped calcrete dolocrete nodules with hard nodule clusters in places, fewer nodules from 131.07 to 131.33 m	
-133	1	0	Fine to very fine sand as above, minor silt, very clayey but variable clay content, very minor medium sand clayey but variable clay content, v miner ms, green, soft & hard in places; abundant small to medium irregular shaped calcrete dolocrete nodules with hard nodule clusters in places;	
-134	1	0	Fine to very fine sand as above, minor silt, very clayey but variable clay conent,very minor medium sand, it's green,hard,with abundant small to medium irregular shaped calcrete dolocrete nodules with more hard nodule clusters;	Darker green 2nd period bioturbidation channels in the sand between the nods
-135	0.94	0.06	Same as above to 134.21 m, then bigger irregular, vertically elongate calcrete dolocrete nodules more widely spaced in hard very light green to very light grey-green clayey sand to 134.84 m, then almost no nodules	2 reddish bioturbidation channels at 134.9 m

Depth to m	Core recovery m	Core loss m	Core description	Bioturbation
-136	1	0	Sand as above, very light green to very light grey-green, slight darker green from 135.3-135.9 m, possibly faint horizontal bedding to 1356.09 m & from 135.78-135.96 m, soft below about 135.7 m, fewer and smaller nodules, clayey sand variable calcrete	Faint reddish bioturbidation channels from 135.3-135.42 m, thin calcified rhyzolith at 135.42 m, some small round or elongate nodules may be calcified bioturbidation channels
-137	1	0	Sand as above, very clayey possibly becoming more clayey downwards, non calcrete, sand soft, scattered irregularly shaped calcrete dolocrete nodules of various sizes, ± 60% sand, 40% nodules, no nodules between 136.76 & 136.88 m	Possibly some very faint bioturbidation
-138	1	0	Clay, minor silt, fine sand, non calcrete; a few small calcrete dolocrete nodules	Faint, abundant bioturbidation channels in lower 30 cm, of light green bioturbidation in very light brown sand or vice versa, a thin calcified rhyzolith at 137.93 m

Depth to m	Core recovery m	Core loss m	Core description	Bioturbation
-139	1	0	Clay as above to 138. Fine to very fine sand, minor silt, very clayey but variable clay content, very minor medium, rare coarse grains at 138.13 m, poor sorting, soft, green but becomes whiter & Lighter green & harder where abundant calcrete dolocrete nodules due to matrix cementing; small irregular shaped, often longish calcrete dolocrete nodules throughout but zones of concentrated nodules from 138.20-128.32, 138.64-138.92 m. 2 large white irregularly shaped silcrete nodules at 138.51 m. no nodules below 139.96 m	White, thin, rhyzolith-like features filled with calcrete dolocrete at 138.30 (zoned), 138.37, 138.56, 138,71, 138.82, 138.87 m
-140	1	0	Fine to very fine sand, minor silt, very clayey to 139.4 m, soft, green; clay non calcrete; patches of calcrete dolocrete nodules from 139.4-139.6, 139.72-139.83, 139.88-140 m; 1 white chert nodule at 139.1 m	bioturbidation-sized patches of sandy clay and clayey sand probably due to bioturbidation
-141	1	0	Fine to very fine sand ,minor silt, very clayey, becomes much more clayey below 140.4 m, soft, green; non calcrete to silcrete calcrete; a few scattered fairly large calcrete dolocrete nodules, 1 large nodule at 140.5 m; possible very faint horizontal bedding at 140.68 m, and slight angled bedding from 140.83-140.93 m	

Depth to m	Core recovery m	Core loss m	Core description	Bioturbation
-142	1	0	141-141.40 m:- Sand as above, very clayey, green, non to slight calcrete, soft, scattered irregular-shaped white calcrete dolocrete nodules 141.40-141.73 m:- as above but with faint purplish more clay-rich patches; same calcrete dolocrete nodules 141.73-142 m:- Clay, deep grey-purple, one small calcrete dolocrete nodule near base	141-141.40 m:- some slight reddish bioturbidation; 141.40-141.73 m:- mixed green & purple clay due to bioturbidation, some 2nd period red bioturbidation near base 141.73-142 m:- some faint reddish sand-filled bioturbidation channels, no deep red
-143	1	0	142-142.26 m:- Clay as above, deep grey-purple, small calcrete dolocrete nodules; 142.26-142.40 m:- Transition downwards to underlying light green sand through gradual decrease in clay content and decrease in purple colour; 142.40-143 m: fine Sand, minor silt, clay, light green, soft, non calcrete, a few small irregular-shaped calcrete dolocrete nodules; lt's purple zone from 142.75-142.84 m, sand more clayey below this	142-142.26 m:- fewer of above bioturbidation channels; 142.40 m:- 2 red bioturbidation channels

Depth to m	Core recovery m	Core loss m	Core description	Bioturbation
-144	1	0	Sand as above to 143 m, rare coarse grains, clay content possibly decreasing downwards, much less clay below 143.57 m, soft, small irregularly-shaped calcrete dolocrete nodules	Some faint reddish bioturbidation channels in basal 10 cm
-145	1	0	Fine sand, minor silt, clay, light green, soft, non calcrete, a few small irregularly-shaped calcrete dolocrete nodules;	A few 1st period light purple bioturbidation channels scattered through core, fewer 2nd period red bioturbidation channels; one calcrete-filled rhyzolith(?) at 144.65 m
-146	1	0	Same as above; fewer nodules	Faint 1st period lt's purple scattered through core, clear red 2nd period bioturbidation at 145.44 m, one zoned with red rim, light green sand core
-147	1	0	Same as above; fewer nodules	No obvious bioturbidation

Depth to m	Core recovery m	Core loss m	Core description	Bioturbation
-148	0.9	147-148.1	Same as above, rare medium sand and coarse grains, very light green, soft; only 1 calcrete dolocrete nodules -at 147.25 m	A few faint light purple bioturbidation channels scattered through core; long zoned light purple channels with white rim in middle part; 4 tiny widely spaced red bioturbidation channels
-149	1	0	Same as above, large calcrete dolocrete nodules with cavities at 148.3 m, large nodules forms the last 15 cm of this core	Faint light purple bioturbidatio throughout, these channels clustered at 148.53 m
-150	1	0	Last nodule of above core continues to 149.16 m; 149.16-149.89 m:Fine to very fine, minor silt , very minor clay, poor sorting, very light yellow soft; rare calcrete dolocrete nodules 149.89-149.94 m:Fine sand, minor silt, clayey, poor sorting, light green; 149.94-150 m:- calcrete dolocrete nodule	Faint light purple bioturbidation throughout, red bioturbidation in places in very light yellow sand; white bioturbidation channels at 149.74 m. Purple and red bioturbidation in light green sand

Appendix 2: Cumulative frequency curves for grain size analysis

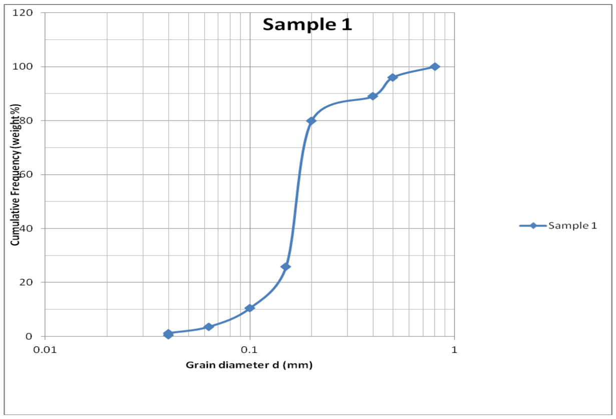

Cumulative Frequency curve for Sample 1

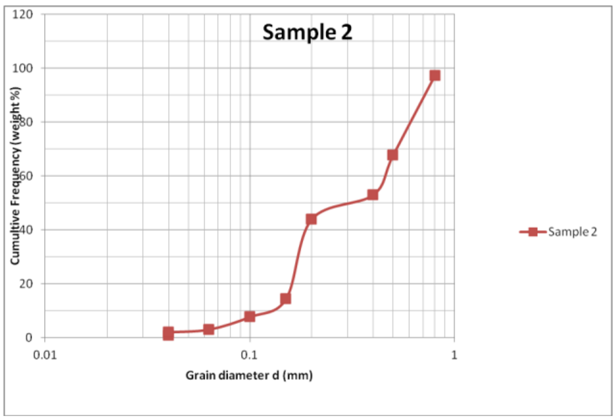

Cumulative Frequency curve for Sample 2

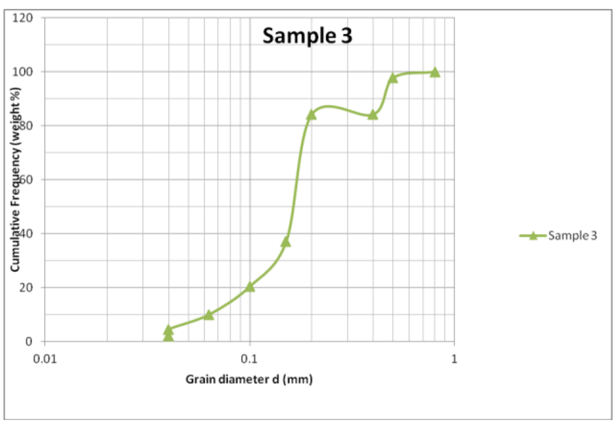

Cumulative Frequency curve for Sample 3

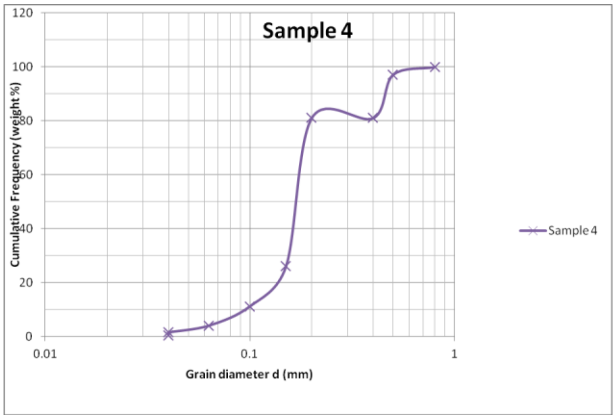

Cumulative Frequency curve for Sample 4

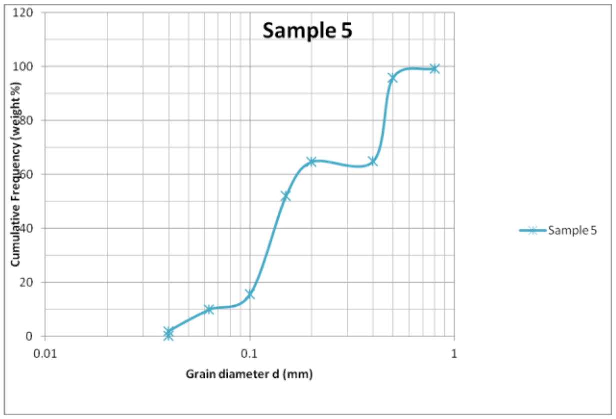

Cumulative Frequency curve for Sample 5

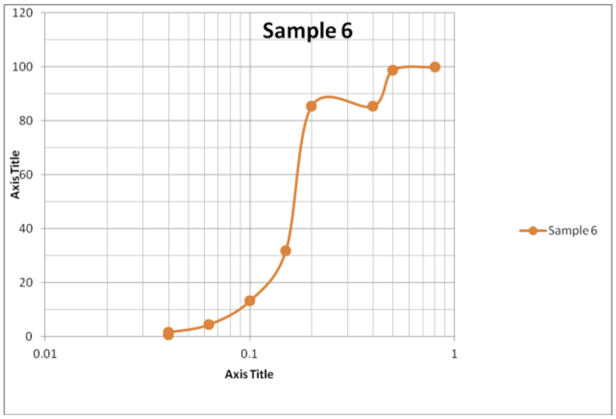

Cumulative Frequency curve for Sample 6

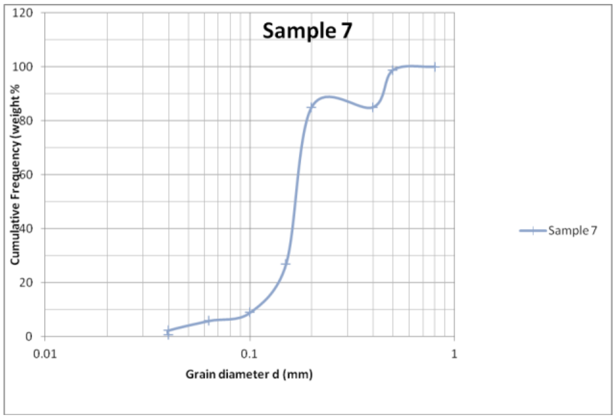

Cumulative Frequency for Sample 7

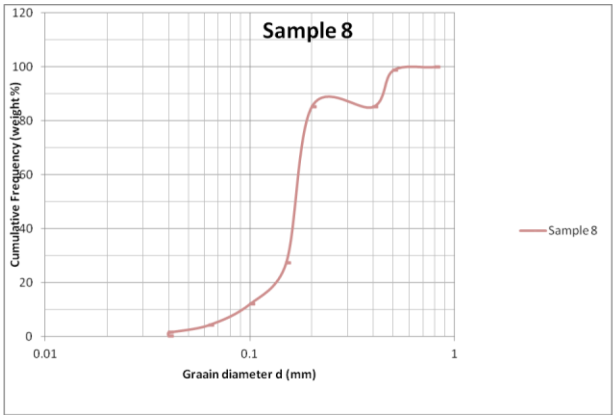

Cumulative Frequency curve for Sample 8

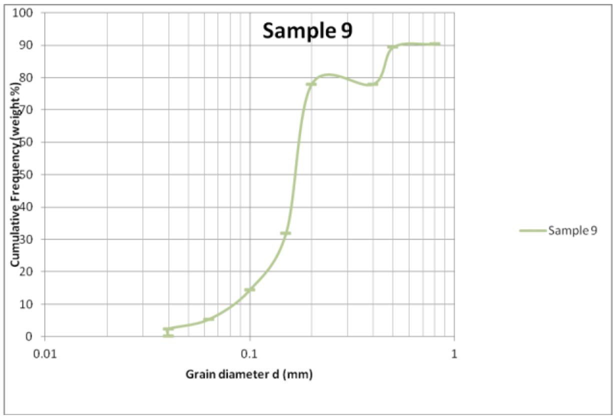

Cumulative Frequency curve for Sample 9

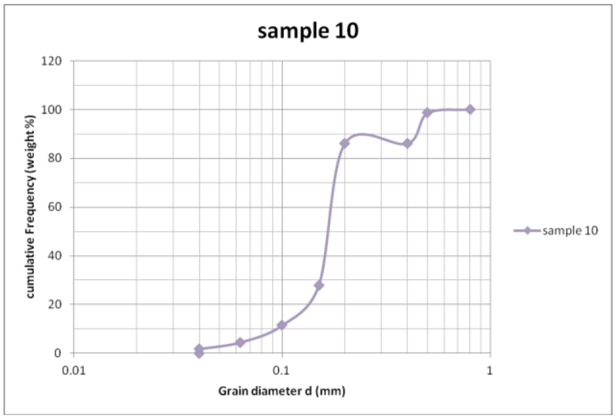

Cumulative Frequency curve for Sample 10

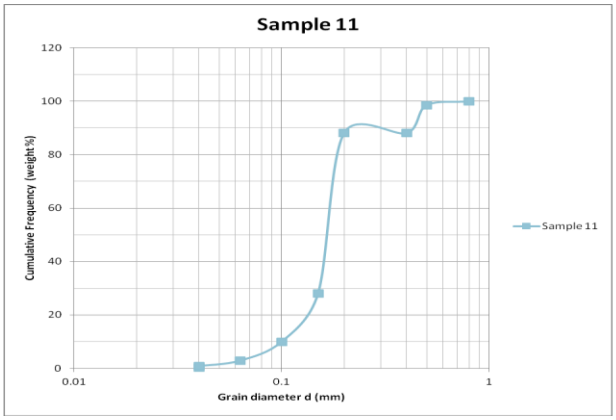

Cumulative Frequency curve for Sample 11

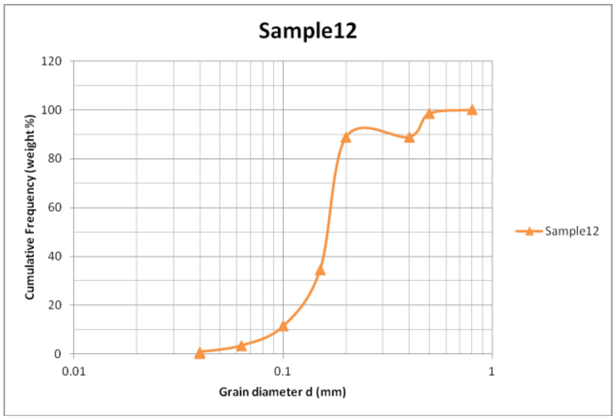

Cumulative Frequency curve for Sample 12

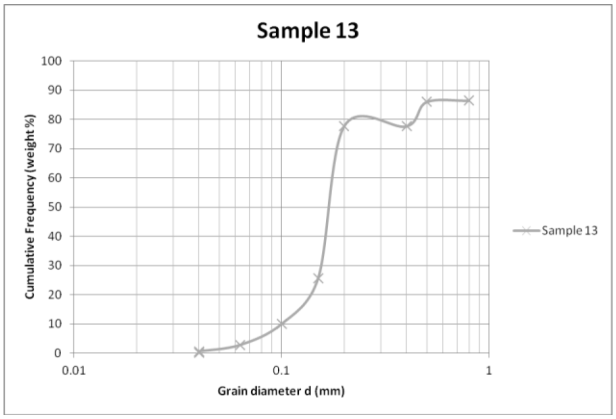

Cumulative Frequency curve for Sample 13

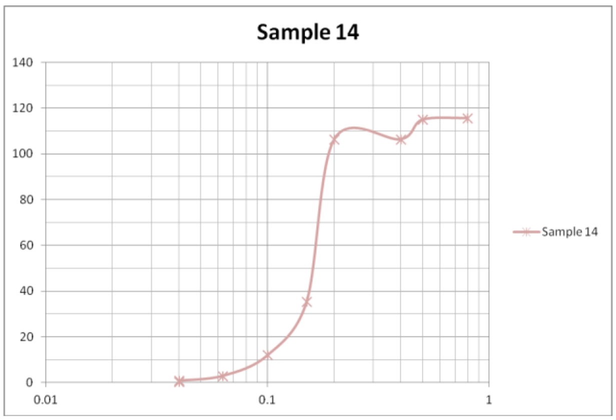

Cumulative Frequency curve for Sample 14

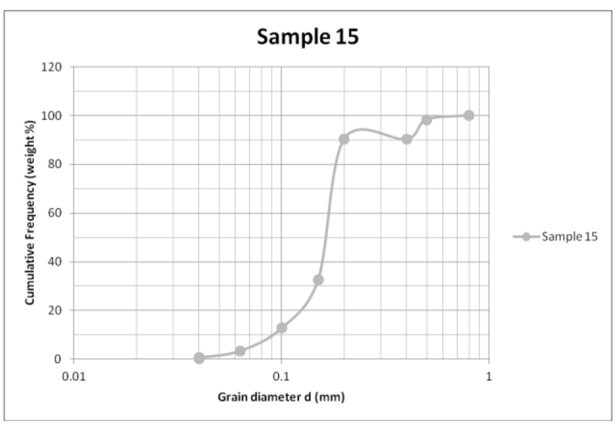

Cumulative Frequency curve for Sample 15

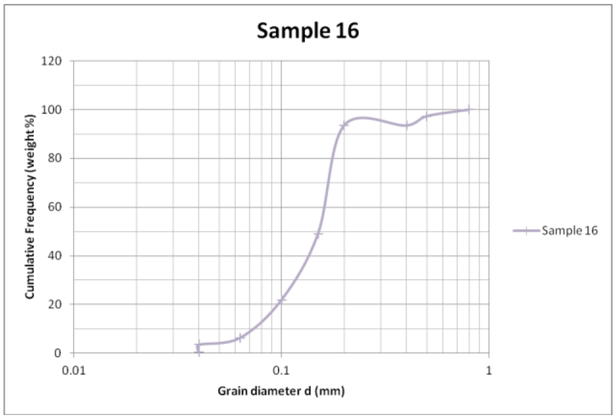

Cumulative Frequency curve for Sample 16

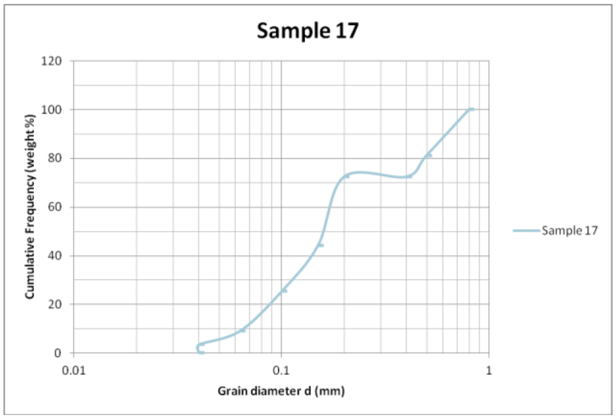

Cumulative Frequency curve for Sample 17

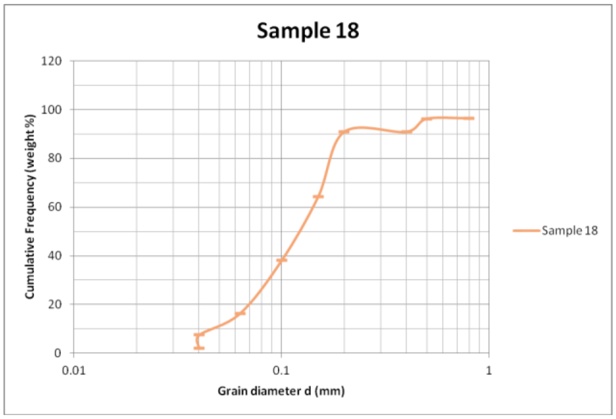

Cumulative Frequency curve for Sample 18